ATLAS PREPRINT

March 8, 2011

Measurements of underlying-event properties using neutral and charged particles in pp collisions at $\sqrt{s} = 900$ GeV and $\sqrt{s} = 7$ TeV with the ATLAS detector at the LHC

The ATLAS Collaboration

Abstract

We present first measurements of charged and neutral particle-flow correlations in pp collisions using the ATLAS calorimeters. Data were collected in 2009 and 2010 at centre-of-mass energies of 900 GeV and 7 TeV . Events were selected using a minimum-bias trigger which required a charged particle in scintillation counters on either side of the interaction point. Particle flows, sensitive to the underlying event, are measured using clusters of energy in the ATLAS calorimeters, taking advantage of their fine granularity. No Monte Carlo generator used in this analysis can accurately describe the measurements. The results are independent of those based on charged particles measured by the ATLAS tracking systems and can be used to constrain the parameters of Monte Carlo generators.

To be submitted to *EPJ C*

1 Introduction

All hard parton-parton interactions in pp collisions are accompanied by additional processes which collectively contribute additional particles to those from the hard scatter and which are termed the underlying event (UE). It is impossible to uniquely separate the UE from the hard scattering process on an event-by-event basis. However, observables can be measured which are sensitive to properties of the UE. In order to make high-precision measurements, the UE must be modelled using phenomenological models in Monte Carlo generators [1]. Such models must be tuned to experimental data. In the past, such studies have only been performed using tracks [2–4].

Many physics processes to be studied with the ATLAS detector [5] require precision measurements of jets and missing transverse energy obtained principally from the calorimeter system. Therefore, it is important that the UE measurements are performed using the same instrumental environment and reconstructed objects as those for the calorimeter-based measurements. The fine granularity of the ATLAS calorimeter allows the definition of three-dimensional clusters of energy which are closely associated with individual particles [6, 7].

A study of the UE using charged-track densities was recently performed by ATLAS [4]. The present paper extends this measurement by reconstructing particle densities using calorimeter clusters in the region which is most sensitive to the soft QCD processes responsible for the UE; the "transverse" region as shown in Fig. 1. The azimuthal angular distance between a leading particle in transverse momentum (p_{T}) and other particles is given by $\Delta\phi = \phi - \phi_{\mathrm{lead}}$, where ϕ is the azimuthal angle of a particle and ϕ_{lead} is the azimuthal angle of the leading particle. The transverse region, defined as $60^\circ < |\Delta\phi| < 120^\circ$, is most sensitive to the UE since it is perpendicular to the axis of hardest scattering, approximated by the direction of the leading particle. As is the case for charged particles, the number density of the clusters and their transverse energy density in this region are sensitive, discriminating observables for UE studies. These distributions are corrected for detector effects to give a measure of the particle activity in the UE and to provide new characteristics which can be used to tune models included in Monte Carlo generators.

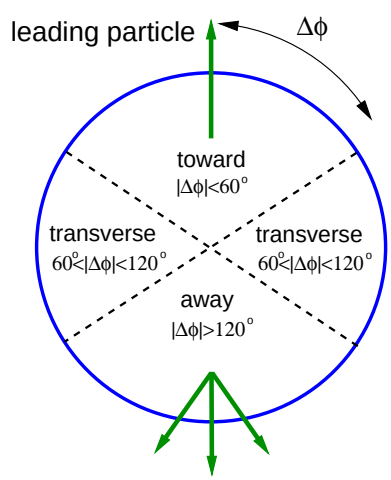

Figure 1: A schematic representation of regions in the azimuthal angle ϕ with respect to the leading particle (shown with the arrow). In this analysis, the leading particle corresponds to the cluster with the largest transverse momentum.

The analysis using calorimeter clusters has several important features. Firstly, its results are sensitive to the entire hadronic final state, including neutral particles, which constitute about 40% of all produced particles. Secondly, the analysis based only on calorimeter clusters has completely independent exper-

imental uncertainties compared to the corresponding analysis [4] using charged particles. Finally, as discussed earlier, since jet reconstruction is based almost entirely on energy deposition in the calorimeter, the results of this UE analysis can be used directly to estimate the effect of the underlying event on any jet-based measurement.

2 The ATLAS Detector

The ATLAS detector [5] at the Large Hadron Collider was designed to study a wide range of physics. It covers almost the entire solid angle around the collision point with layers of tracking detectors, calorimeters and muon chambers.

Charged tracks and vertices are reconstructed with the inner detector which consists of a silicon pixel detector, a silicon strip detector and a transition radiation tracker, all immersed in a 2 tesla magnetic field provided by a superconducting solenoid. For the measurements presented in this paper, the high-granularity calorimeter systems are of particular importance. The ATLAS calorimeter system provides fine-grained measurements of shower energy depositions over a large range in pseudorapidity[1]. Electromagnetic calorimetry in the range $|\eta| < 3.2$ is provided by liquid argon (LAr) sampling calorimeters. This calorimeter system provides measurements of the shower energy in up to four depth segments and with transverse granularity that ranges from 0.003×0.10 to 0.05×0.025 in $\delta\eta \times \delta\phi$, depending on depth segment and rapidity. The hadronic calorimetry in the range $|\eta| < 1.7$ is provided by a steel/scintillator-tile sampling calorimeter. This system provides measurements of the shower energy deposition in three depth segments at a transverse granularity of typically 0.1×0.1. In the end-caps ($|\eta| > 1.5$), LAr technology is used for the hadronic calorimeters that match the outer η limits of the end-cap electromagnetic calorimeters. This system provides four measurements in depth of the shower energy deposition at a transverse granularity of either 0.1×0.1 ($1.5 < |\eta| < 2.5$) or 0.2×0.2 ($2.5 < |\eta| < 3.2$). The LAr forward calorimeters provide both electromagnetic and hadronic energy measurements and extend the calorimeter coverage from $|\eta| = 3.2$ to $|\eta| = 4.9$. To measure the energy of photons and electrons, all calorimeter cells are initially calibrated to the electromagnetic energy scale using test-beam data [8, 9].

This analysis is based on the properties of topological clusters in the calorimeter, which represent an attempt to reconstruct three-dimensional energy depositions associated with individual particles [6, 7]. The topological-cluster algorithm proceeds through the following steps. Nearest neighbours are collected around seed cells, which are cells with an absolute signal greater than 4σ above the noise level [8, 9]. Then, neighbouring cells are collected into the cluster if the absolute value of their signal significance is above a secondary seed threshold of 2σ. All surrounding cells are iteratively added to the cluster until no further secondary seeds are among the direct neighbours. A final analysis of the resulting cluster looks for multiple local signal maxima; in the case of more than one maximum in a given cluster, it is split into smaller clusters along the signal valleys between the maxima.

The analysis presented in this paper uses calibrated topological clusters [7]. The clusters are classified as related to electromagnetic or hadronic energy deposits, using detailed information on the cluster topology. Then, the reconstructed cluster energy is corrected for the non-compensating nature of the ATLAS calorimeter and for inactive material.

[1] The ATLAS reference system is a Cartesian right-handed co-ordinate system, with the nominal collision point at the origin. The anti-clockwise beam direction defines the positive *z*-axis, while the positive *x*-axis is defined as pointing from the collision point to the centre of the LHC ring and the positive *y*-axis points upwards. The azimuthal angle ϕ is measured around the beam axis, and the polar angle θ is the angle measured with respect to the *z*-axis. The pseudorapidity is given by $\eta = -\ln\tan(\theta/2)$. Transverse momentum is defined relative to the beam axis.

3 Data selection

The data taken at $\sqrt{s} = 900$ GeV were collected during 6–15 December 2009. During this running period, there were approximately 3% non-functional channels in the tile hadronic calorimeter and approximately 1% non-functional channels in the LAr calorimeters [9]. For an integrated luminosity of 7 μb^{-1}, a total of 455 thousand events were collected from colliding proton bunches in which a minimum-bias trigger recorded one or more hits in the scintillators on either side of the detector.

The events to be analysed were selected using a procedure identical to that described in Refs. [4, 10]. Events were required to have a primary vertex which is reconstructed using at least two tracks with transverse momenta $p_{\mathrm{T}} > 100$ MeV and a transverse distance of closest approach with respect to the beam-spot position [11] of less than 4 mm.

This analysis uses topological clusters with $p_{\mathrm{T}} > 0.5$ GeV and $|\eta| < 2.5$ in order to have the same kinematic range[2] as for the previous UE study based on tracks [4]. Additional selection criteria were applied to select good-quality clusters: 1) to reject the cosmic and noise background, the leading cell energy of the cluster is required to be less than 90% of the cluster energy; 2) the energy sampling maximum must be in a calorimeter region with good calibration; 3) the fraction of energy in the cluster associated with problematic cells (or dead cells where the energy contribution is obtained by interpolation from adjacent cells) should be less than 50%.

Data at $\sqrt{s} = 7$ TeV were collected between 30 March and 27 April 2010. Only a fraction of the 7 TeV data, corresponding to an integrated luminosity of about 230 μb^{-1}, was used. In total, about 7.7 million events were analysed. Event selection was similar to that for the 900 GeV data, but included the additional requirement of a single primary vertex [4, 10] to remove events containing more than one pp interaction.

4 Monte Carlo simulation

The QCD predictions for the hadronic final state in inelastic pp collisions are based on several Monte Carlo generators. The PYTHIA 6.4 Monte Carlo generator [12] is used as the primary generator for comparisons with the data. The MC09 tune [13] of this model was performed by ATLAS. It uses the p_{T}-ordered parton shower with the MRST LO* parton-density function [14], followed by fragmentation into final-state particles using the Lund string model [15]. The parameters of this generator were adjusted to describe charged-particle multiplicity distributions in minimum-bias events measured at $\sqrt{s} = 630$ GeV and $\sqrt{s} = 1.8$ TeV in $p\bar{p}$ collisions [16]. Diffractive processes are not included in the simulation for the main samples, but were used for systematic checks (Sect. 7). In addition to the MC09 tune, the following two PYTHIA parameter sets are also used: (1) the Perugia0 set [17] in which the soft-QCD part is tuned using only minimum-bias data from the Tevatron and CERN $p\bar{p}$ colliders; (2) the DW [18] PYTHIA tune, which uses virtuality-ordered showers and was derived to describe the CDF Run II underlying event and Drell-Yan data.

The data are also compared to the PHOJET Monte Carlo generator [19], which includes a simulation of the diffractive component. This generator is based on the two-component Dual Parton Model which includes soft hadronic processes described by Pomeron exchange and semi-hard processes described by perturbative parton scattering. The description of the fragmentation is the same as in the PYTHIA generator.

In addition, the HERWIG Monte Carlo generator [20, 21] was used for comparisons with the data. This generator has similar matrix-element calculations as PYTHIA, but uses the cluster fragmentation

[2] The topological clusters are treated as massless particles, and we choose to refer to both clusters and stable particles in terms of p_{T}. The same symbol p_{T} is also used to represent the track transverse momentum.

model to hadronise partons into hadrons. HERWIG is interfaced with the JIMMY model [22] in order to describe multiple parton interactions.

Monte Carlo events were processed through the ATLAS detector simulation program [23], which is based on GEANT4 [24]. They were reconstructed using the same trigger and event selection as for the data. The size and position of the collision beam-spot and the detailed description of detector conditions during the data-taking runs were included in the simulation.

Monte Carlo events after the detector simulation program were used for correcting the data to the stable-particle level defined as follows. The PYTHIA MC09 is used to generate the primary samples for unfolding the effects of the detector. Monte Carlo stable particles are selected if their mean lifetimes are larger than $3 \cdot 10^{-11}$ seconds. Neutrinos are excluded from consideration. According to this definition, K_S^0, Λ and $\Sigma^{\pm}$ are among those treated as stable particles. This definition allows a direct comparison between the results of previous track-based studies [4] and the present measurement.

5 Properties of calorimeter clusters

Figures 2 and 3 show the distributions of p_{T} and η for topological clusters in data and simulated PYTHIA MC09 events at $\sqrt{s} = 900$ GeV and $\sqrt{s} = 7$ TeV, respectively. The distributions in each case are normalised to the number of entries. In addition, the ratio plots show the ratio of simulation to data in the transverse region alone. The figures show overall good agreement between the data and the PYTHIA MC09 tune, with 20% discrepancies in some phase-space regions. While not shown in these figures, the Perugia0 tune agrees with the data to a similar extent. The contribution of the discrepancy in the high-p_{T} tail is expected to be small on particle densities measured at $p_{\mathrm{T}} > 0.5$ GeV, and it was taken into account using re-weighting as described below. The observed differences between the data and the PYTHIA MC09 event sample for the η distributions are addressed in the studies of systematic uncertainties.

Figures 4(a) and 5(a) show the multiplicity of topological clusters, with $p_{\mathrm{T}} > 0.5$ GeV and $|\eta| < 2.5$, versus the number of stable particles (charged and neutral) in simulated events for $\sqrt{s} = 900$ GeV and $\sqrt{s} = 7$ TeV. A strong correlation is observed between the number of topological clusters and the number of stable particles, indicating that clusters are a good representation of the particle activity in inelastic pp events.

Figures 4(b) and 5(b) show the correlation between the number of topological clusters and the number of primary tracks selected in the same way as in the track-based studies [4, 10]. These figures also show a strong correlation. The Monte Carlo simulation shown in Fig. 4(c) and 5(c) reproduces these distributions well: the means and the root-mean-square deviations of one-dimensional projections of these distributions agree with the Monte Carlo simulation within less than one percent for $N(\text{tracks}) > 4$. For events with a lower number of tracks, the data show a smaller mean value of the projection onto the x-axis than seen in the PYTHIA MC09 simulation. This is attributed to the absence of diffraction in the generated samples.

A Monte Carlo simulation study based on PYTHIA MC09 indicates that the probability that a second particle lies within $\sqrt{\delta\eta^2 + \delta\phi^2} < 0.2$ of a first in the selected inelastic pp events is below 1%. This simplifies the present analysis since there is negligible potential bias due to cluster overlap.

For the UE studies based on topological clusters, a good position measurement is required. The quality of the position reconstruction of the clusters was studied by comparing the impact point of charged particles with the associated cluster position in the calorimeter. Charged particles are deflected in the magnetic field of the solenoid. Their trajectories are extrapolated to the calorimeter using a Monte Carlo simulation which includes a detailed field map as well as the effect of the material in front of the calorimeter. The Monte Carlo simulation describes the topological-cluster positions relative to the positions of the extrapolated tracks on the surface of the LAr calorimeter within the granularity of its second layer (0.025×0.025 in $\delta\eta \times \delta\phi$).

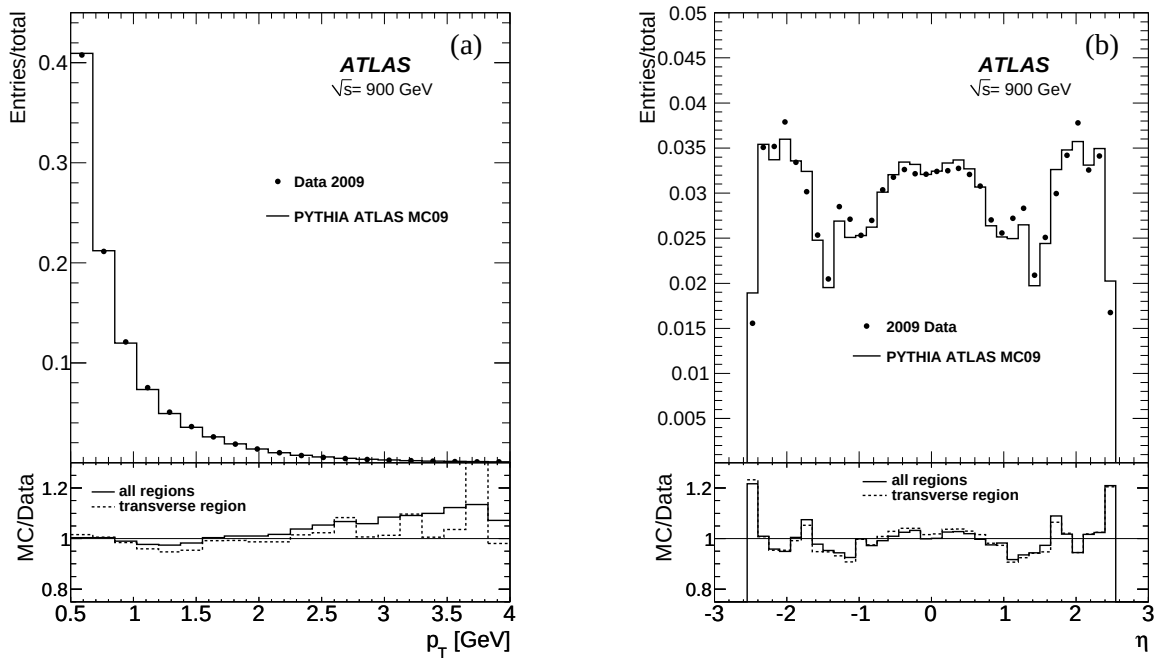

Figure 2: A comparison between uncorrected data and the Monte Carlo simulation for topological cluster p_{T} (a) and η (b) for pp collisions at $\sqrt{s} = 900$ GeV. The ratio plots show the inclusive sample (solid lines) and the transverse region (dashed lines).

As the correction for detector effects is based on the Monte Carlo simulation, an essential issue is the accuracy with which the simulation reproduces the energy reconstruction in the calorimeter. For charged particles, the energy scale was studied [25,26] using isolated tracks by extrapolating tracks to the calorimeter surface and matching them to topological clusters. The average value of the ratio E/p was reconstructed, where E is the cluster energy in the calorimeter and p is the track momentum. Figure 6 shows the average response $\langle E/p \rangle$ for calibrated topological clusters as a function of η for tracks with $p > 0.5$ GeV. The data and PYTHIA MC09 agree within 5% in most η regions, while discrepancies increase in the transition region ($1.5 < |\eta| < 1.8$) between barrel and end-cap.

To estimate the relative energy-scale uncertainty, the double ratio $\langle E/p \rangle_{MC} / \langle E/p \rangle$ was calculated, where the ratio $\langle E/p \rangle_{MC}$ was determined from the Monte Carlo simulation. The double ratio as a function of η is shown in Fig. 6 (bottom). The double-ratio distributions were measured for a wide range of track momenta and η as described in Refs. [25, 26].

The comparison between data and Monte Carlo predictions for the shapes of the E/p distribution is shown in Fig. 7. The peak at zero corresponds to isolated tracks that have no associated cluster in the calorimeter. These are predominantly due to hadronic interactions in the material in front of the calorimeter [26]. The contribution of the discrepancies observed for $E/p = 0$ between the data and PYTHIA MC09 to uncertainties on the reconstruction efficiencies of topological clusters is below 1%. This effect was taken into account as described in Sect. 7. More details on the energy scale of topological clusters can be found in Refs. [25, 27].

The energy scale for electromagnetic clusters was estimated using the π^0 peak reconstructed in inelastic pp events. The selection criteria for calibrated topological clusters were the same as for the present analysis. The π^0 peak positions for data and PYTHIA MC09 agree within 3% for all η regions.

Correction of the observed distributions to the particle level requires a reliable description of the cluster multiplicity distribution by the simulated event sample. This was studied by examining cluster

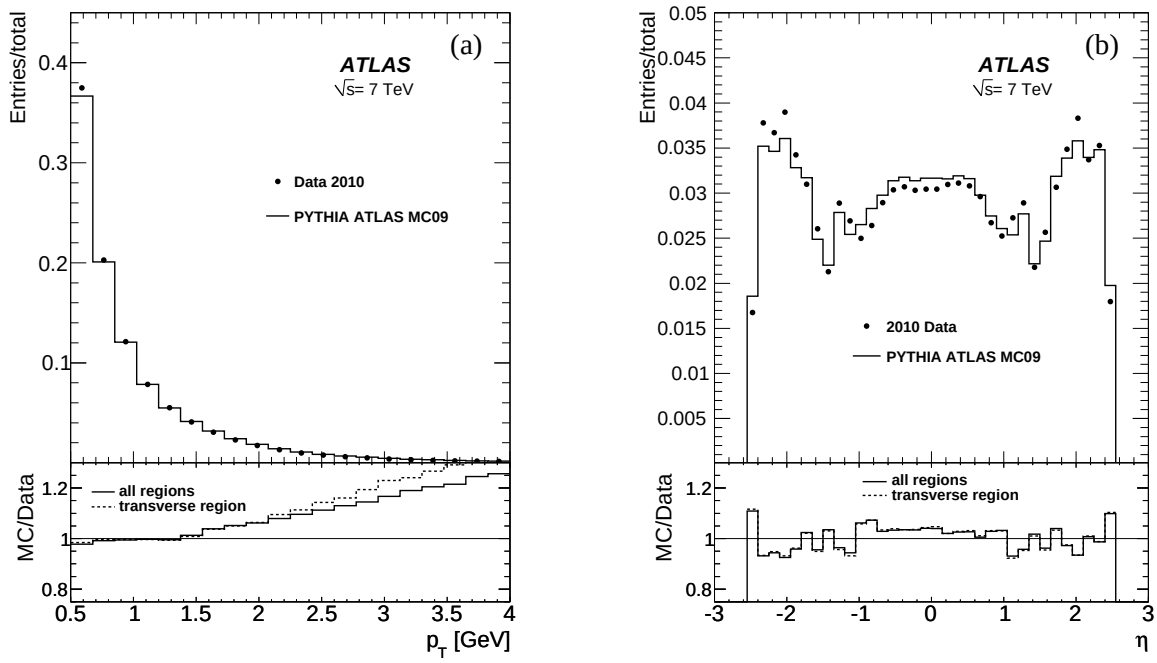

Figure 3: A comparison between uncorrected data and the Monte Carlo simulation for topological cluster p_{T} (a) and η (b) for pp collisions at $\sqrt{s} = 7$ TeV . The ratio plots show the inclusive sample (solid lines) and the transverse region (dashed lines).

multiplicities in bins of track multiplicity using projections of the two-dimensional distributions shown in Figs. 4 and 5. The observed differences are propagated into the systematic uncertainties as discussed in Sect. 7.

For the UE studies, the so-called "leading" clusters, i.e. clusters with the largest transverse momenta, $p_{\mathrm{T}}^{\mathrm{lead}}$, are used to define an event orientation. Such clusters are typically inside the most energetic jets. To verify this, jets were reconstructed with the anti-k_t algorithm [28] with a distance parameter of 0.4, a minimum p_{T} requirement of 5 GeV and $|\eta| < 2.5$. Then, the distance in η–ϕ between the leading topological cluster and the centre of the leading jet was calculated. It was shown that, in the vast majority of cases, the leading cluster is inside a leading jet with only a small fraction ($\simeq 10\%$) of clusters opposite the leading jet in ϕ. This feature is well reproduced by the Monte Carlo simulation.

To verify the Monte Carlo performance for $p_{\mathrm{T}}^{\mathrm{lead}}$, the ratio of $p_{\mathrm{T}}^{\mathrm{lead}}$ of topological clusters to $p_{\mathrm{T}}^{\mathrm{lead}}$ of primary tracks was reconstructed. The agreement between the data and the PYTHIA MC09 tune for such distributions was found to be within $\pm 5\%$ in most regions, while discrepancies at the level of 20% were found for the tails of the ratio distributions. The impact of such discrepancies in the simulation of the $p_{\mathrm{T}}^{\mathrm{lead}}$ resolution on the final measurement has been estimated as discussed in Sect. 7.

Monte Carlo studies show that the rate of events in which a low-p_{T} particle is reconstructed as a high-p_{T} cluster is not negligible. This results in a low purity for topological clusters at high $p_{\mathrm{T}}^{\mathrm{lead}}$. Therefore, the analysis was performed for leading topological clusters with transverse momenta less than 8 GeV (14 GeV) for the $\sqrt{s} = 900$ GeV (7 TeV) data in order to limit this effect and to ensure that the reconstruction purity even at the highest transverse momenta considered is larger than 50%.

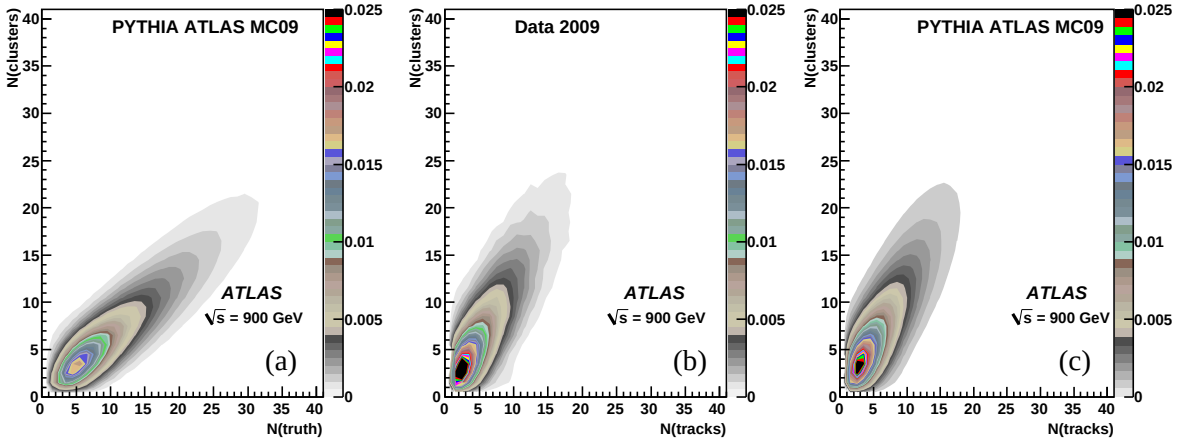

Figure 4: ATLAS data at $\sqrt{s} = 900$ GeV: The correlations between the multiplicities of, (a) topological clusters (N(clusters)) and stable particles (N(truth)) from simulated pp interactions, (b) topological clusters and primary reconstructed tracks (N(tracks)) from pp interactions, and (c) topological clusters and primary reconstructed tracks from simulated pp interactions. Inelastic events generated by PYTHIA MC09 (without diffraction) passed through the selection were used to produce the plots (a) and (c).

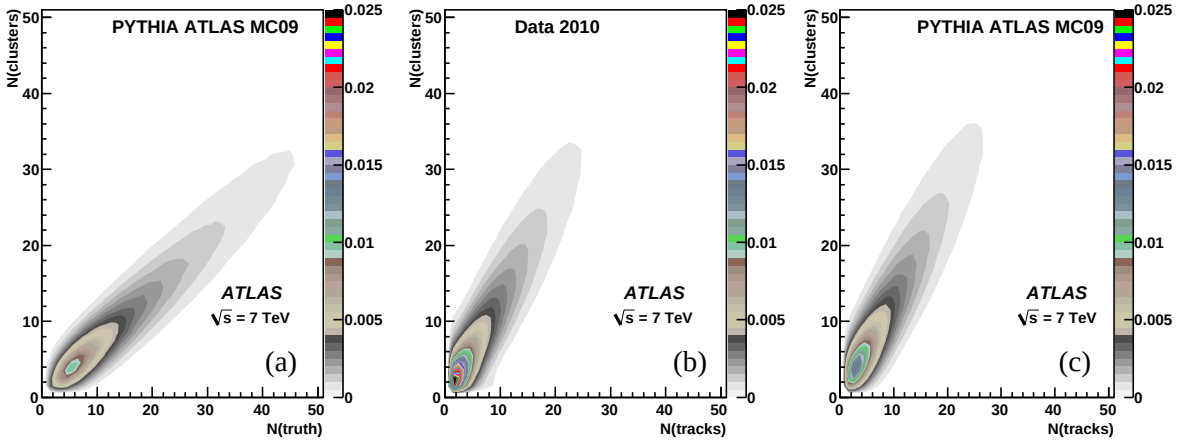

Figure 5: ATLAS data at $\sqrt{s} = 7$ TeV: The correlations between the multiplicities of, (a) topological clusters (N(clusters)) and stable particles (N(truth)) from simulated pp interactions, (b) topological clusters and primary reconstructed tracks (N(tracks)) from pp interactions, and (c) topological clusters and primary reconstructed tracks from simulated pp interactions. Inelastic events generated by PYTHIA MC09 (without diffraction) passed through the selection were used to produce the plots (a) and (c).

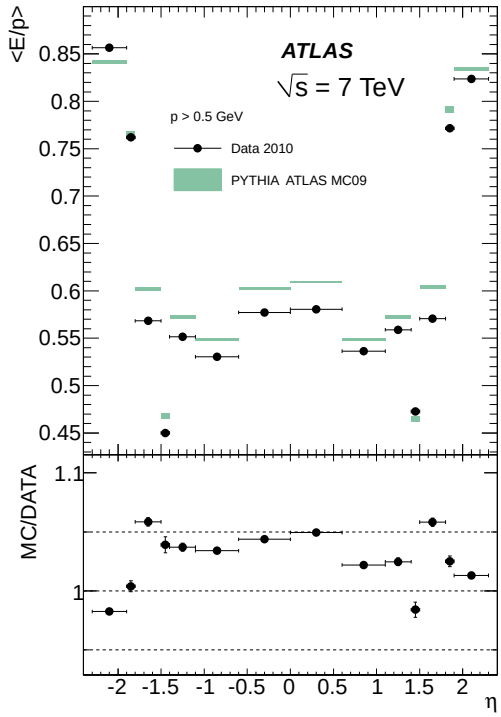

Figure 6: The average E/p in different η bins for isolated topological clusters matched to charged tracks in inelastic pp events at $\sqrt{s} = 7$ TeV for track momentum p larger than 0.5 GeV. A similar level of agreement between data and the Monte Carlo simulation was obtained for the $\sqrt{s} = 900$ GeV data (not shown).

6 Measured observables and correction procedure

Following earlier track-based analyses [4], particle densities are studied as a function of the distance $\Delta\phi$ in the azimuthal angle between the leading cluster and all other clusters in an event, and as a function of p_{T} of the leading cluster in the event. The scalar p_{T} sum for stable particles per unit area in η–ϕ in the transverse region is also presented. This provides complementary information to that which can be obtained from the particle densities.

The particles and clusters are required to have $p_{\mathrm{T}} > 0.5$ GeV and $|\eta| < 2.5$. Clusters are selected if they pass the criteria described in Sect. 3. The measured observables at the particle and detector levels are:

- $p_{\mathrm{T}}^{\mathrm{lead}}$ - Transverse momentum of the stable particle with maximum p_{T} in the event. At the detector level, this corresponds to the transverse momentum of the selected topological cluster with maximum p_{T} in the event.

- $d\langle N\rangle/d\Delta\phi$ - The average number of particles as a function of the azimuthal-angle difference between the leading particle and other particles in an event. The leading particle at $\Delta\phi = 0$ is excluded from this distribution. At the detector level, it corresponds to the mean number of selected topological clusters as a function of the azimuthal-angle distance between the leading topological cluster and other clusters in an event. This density [4] is defined per unit of pseudorapidity as $N/(N_{ev} \cdot (\eta_{\mathrm{max}} - \eta_{\mathrm{min}}))$, where N is the number of entries in $\Delta\phi$ bins, $\eta_{\mathrm{max}} - \eta_{\mathrm{min}} = 5$ represents

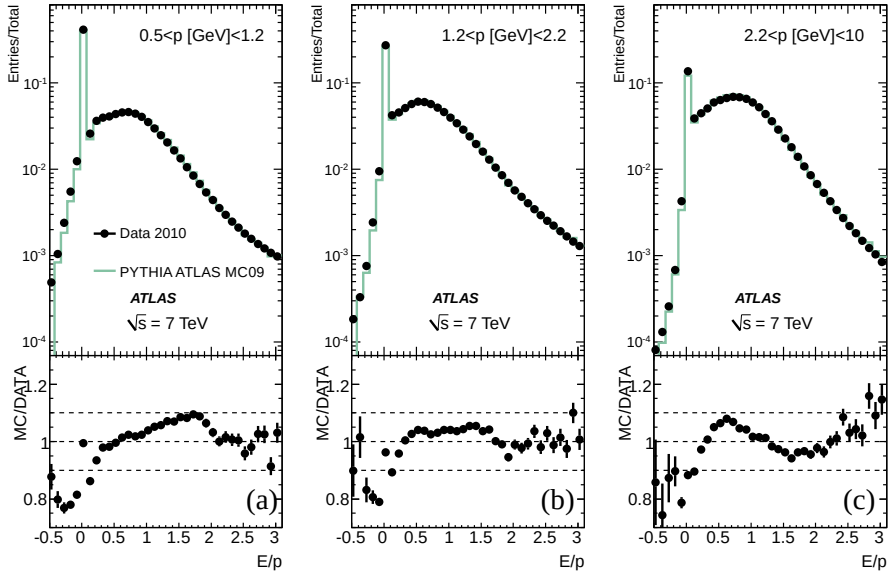

Figure 7: E/p distributions at $\sqrt{s} = 7$ TeV for topological clusters matched to tracks in several bins of track momentum: (a) $0.5 < p < 1.2$ GeV , (b) $1.2 < p < 2.2$ GeV and (c) $2.2 < p < 10$ GeV . The peak at zero corresponds to the events without a good match between a topological cluster and a track. A similar level of agreement between data and Monte Carlo was obtained for the $\sqrt{s} = 900$ GeV data (not shown).

the full pseudorapidity range, and N_{ev} is the number of events selected by requiring a particle with $p_{\mathrm{T}}^{\mathrm{lead}}$ above the specified value.

- $\langle d^2N/d\eta d\phi \rangle$ - Mean number of stable particles per unit area in η–ϕ. At the detector level, this corresponds to the mean number of selected topological clusters per unit area in η–ϕ. This density is measured as a function of $p_{\mathrm{T}}^{\mathrm{lead}}$ [4].
- $\langle d^2\sum p_{\mathrm{T}}/d\eta d\phi \rangle$ - Mean scalar p_{T} sum for stable particles per unit area in η–ϕ. At the detector level, this corresponds to the mean scalar p_{T} sum for selected topological clusters per unit area in η–ϕ. This quantity is defined following the convention used in the previous ATLAS publication [4].

A bin-by-bin correction procedure is used to correct the observed distributions to the stable-particle level. The correction factors

$$C = \frac{\mathscr{A}^{\mathrm{gen}}}{\mathscr{A}^{\mathrm{det}}},$$

are evaluated separately for each observable. In the above expression, $\mathscr{A}^{\mathrm{gen}}$ is calculated at the stable-particle level of PYTHIA MC09 and $\mathscr{A}^{\mathrm{det}}$ is calculated after full detector simulation and reconstruction. The corrected value for an observable is found by multiplying its measured value by the relevant correction factor C. These factors correct the data to the stable-particle level and include the effects of event selection, reconstruction efficiency, bin migrations and smearing, including the case when the leading particle is mis-identified and a cluster corresponding to a sub-leading particle is used to define the event orientation and $p_{\mathrm{T}}^{\mathrm{lead}}$.

The bin-by-bin correction depends on the choice of the Monte Carlo event generator. This affects the efficiency correction (mainly due to variations in particle types) and the purity (different stable-particle

level distributions have different fractions of poorly reconstructed objects in each bin as well as different bin migrations). To reduce the model dependence of the correction procedure, bin-by-bin migrations were minimised by using bin sizes larger than the reconstruction resolutions for the distributions presented. In addition, the analysis was restricted to the $p_{\mathrm{T}}^{\mathrm{lead}}$ ranges where the purity of leading clusters is above 50% (see Sect. 5).

The bin-by-bin correction factors for the particle densities typically have values of around 1.3 and do not exceed 1.4. The largest single contributor is the reconstruction inefficiency of topological clusters, which leads to a bin-by-bin correction factor of approximately 1.2 on average and has a maximum value of 1.3 at low p_{T}. The other significant contributor is the event reorientation which results from inefficiency of the reconstruction of the leading topological cluster in an event. This causes bin migrations, which were studied by replacing the leading cluster $p_{\mathrm{T}}^{\mathrm{lead}}$ by the leading track $p_{\mathrm{T}}^{\mathrm{lead}}(\mathrm{track})$, for which the efficiency is known to be high [4]. The bin-by-bin corrections for the average scalar p_{T} sum have a maximum value of 1.5 for low $p_{\mathrm{T}}^{\mathrm{lead}}$ and decrease to 1.3 for $p_{\mathrm{T}}^{\mathrm{lead}} > 6$ GeV.

To study the contribution from diffractive events, the PYTHIA [12] and PHOJET [19] Monte Carlo generators were used. Non-diffractive inelastic pp events were mixed with single and double diffractive events in accordance with the corresponding generator cross-sections for such processes. The diffractive contribution was found to be below 1% for the $d\langle N\rangle/d\Delta\phi$ densities at $p_{\mathrm{T}}^{\mathrm{lead}} > 1$ GeV in PYTHIA, and almost entirely concentrated at low multiplicities (fewer than four topological clusters). The contribution of diffractive events is larger for $\langle d^2N/d\eta d\phi\rangle$ and $\langle d^2\sum p_{\mathrm{T}}/d\eta d\phi\rangle$ measured at $p_{\mathrm{T}}^{\mathrm{lead}} < 3$ GeV, but becomes negligible for $p_{\mathrm{T}}^{\mathrm{lead}} > 3$ GeV. Diffractive contributions are higher for PHOJET, but their contribution was found to be smaller than the systematic uncertainties on the final measurements. No attempt to subtract diffractive events from the final measurements was made.

7 Systematic uncertainties

The systematic uncertainties on the measured distributions were determined by changing the selection or the analysis procedure and repeating the analysis. The largest uncertainties are described below:

- The following procedure was used to estimate the effect of the relative energy-scale uncertainty on the final measurements. The double ratio $\langle E/p\rangle_{MC}/\langle E/p\rangle$ was calculated for isolated single particles as described in Sect. 5. The effect of the energy-scale uncertainty on the measured densities was found by decreasing and increasing the p_{T} of topological clusters in the Monte Carlo simulation, keeping the same cluster p_{T} in the data. The magnitude of the variation was set by the value of the double ratio calculated in a grid defined in η and p. To simplify the calculation of the systematic uncertainties, a common variation was used for all topological clusters independent of their origin (hadronic or electromagnetic). The effect of the energy-scale uncertainty is significantly larger than that due to the event selection (including trigger) [10].

- The dependence of the bin-by-bin corrections on the detector material description was estimated by recalculating the corrections using two further samples: one with an extra 10% of material in the tracking system, and the other with $\sim 15\%$ additional material in the region $|\eta| > 2$.

- The physics-model dependence of the bin-by-bin corrections was estimated using the Perugia0 tune [17] instead of PYTHIA MC09. This uncertainty was symmetrised.

- A comparison of multiplicities of topological clusters in bins of track multiplicities indicated some discrepancy between data and Monte Carlo for events with low track multiplicities (see Sect. 5). To estimate a systematic uncertainty to account for this discrepancy, the bin-by-bin acceptance corrections were calculated after re-weighting the PYTHIA MC09 detector-level distributions. For

Check	$d\langle N\rangle/d\Delta\phi$	$\langle d^2N/d\eta d\phi\rangle$	$\langle d^2\sum p_T/d\eta d\phi\rangle$
Energy scale	$\pm4.3\%$	$\pm4\%$	$\pm5.6\%$
Additional material	$+3.5\%$	$+3\%$	$+3.6\%$
Model dependence	$\pm3.5\%$	$\pm5\%$	$\pm4.5\%$
Multiplicity reweighting	$\pm4.5\%$	$\pm10\%$	$\pm11\%$
Resolution reweighting	$\pm0.4\%$	$\pm6\%$	$\pm6\%$

Table 1: A summary of the most important systematic uncertainties. The table lists the values of contributions from different groups of systematic checks. Only the largest values are shown, taken from the bins with the largest effect when the systematic variation was applied.

this, cluster multiplicity distributions were measured in bins of track multiplicity and re-weighting factors were calculated by taking the ratio of the above distribution in data and PYTHIA MC09. The re-weighting procedure also addresses the uncertainties on the noise description used in the Monte Carlo simulation and other effects related to the cluster-reconstruction efficiencies.

- A systematic uncertainty was estimated to account for differences in the p_{T} resolution of leading topological clusters in data compared to the Monte Carlo expectation. Discrepancies in the tails of the distributions of $p_{\mathrm{T}}^{\mathrm{lead}}(\mathrm{clusters})/p_{\mathrm{T}}^{\mathrm{lead}}(\mathrm{tracks})$ were used to extract weighting factors, which were then used to recalculate the acceptance corrections.

Table 1 shows the values of the systematic uncertainties discussed above as a percentage of the measured values. Only the largest values are shown for the bins with the most significant effect from the selection variations or change in the experimental procedure.

In addition to these uncertainties, the following systematic variations were also included: 1) in order to reduce the contribution from diffractive events, the measurement was repeated after removing events with fewer than four clusters; 2) the positions of cluster centres in η and ϕ were shifted by the size of one cell; 3) an alternative model (FTFP-Bertini) for the hadronic-shower simulation in GEANT4 was used to extract the correction factors; 4) the calorimeter transition region of $0.94 < |\eta| < 1.06$, which is not well described by the Monte Carlo simulation was removed in the data and in the simulated PYTHIA MC09 sample. These variations each give systematic uncertainties below 2%, with the exception of that for diffractive events which indicate a $7-10\%$ systematic uncertainty for the $\langle d^2N/d\eta d\phi\rangle$ and $\langle d^2\sum p_{\mathrm{T}}/d\eta d\phi\rangle$ densities measured at $p_{\mathrm{T}}^{\mathrm{lead}} < 3$ GeV. As an additional systematic check, the measurement was also repeated using topological clusters at the electromagnetic energy scale and similar differences between data and Monte Carlo simulations were observed.

The overall systematic uncertainty was determined by adding the above uncertainties in quadrature.

8 Results

Figure 8 shows the density distribution $d\langle N\rangle/d\Delta\phi$ of stable-particles as a function of the distance in azimuthal angle between the leading particle and other particles in an event for $\sqrt{s} = 900$ GeV. This density, defined in Sect. 6, is calculated for events selected by requiring a particle with $p_{\mathrm{T}}^{\mathrm{lead}}$ above the values indicated on the figure. The detector correction for this density is discussed in Sect. 6. The total uncertainty, computed from the addition of statistical and systematic uncertainties in quadrature, is shown as a shaded band on all measurements.

The angular distribution shown in Fig. 8 has a peak at $\Delta\phi \simeq 0$ which reflects the particle activity from the hard interaction. The peak narrows as $p_{\mathrm{T}}^{\mathrm{lead}}$ increases. The shape of this distribution is similar to that observed in the recent track-based publications [2–4], and also similar to the transverse-momentum flow around jets observed at a lower $p\bar{p}$ collision energy [29]. The particle densities measured using

topological clusters are higher than the charged-particle densities measured using tracks [4], which is expected from the neutral-particle contribution.

Figure 9 shows the $\Delta\phi$ density distributions for $\sqrt{s} = 7$ TeV. The distributions show narrower peaks, for a given $p_{\mathrm{T}}^{\mathrm{lead}}$ threshold, than for the $\sqrt{s} = 900$ GeV data.

The data are compared to the PYTHIA Monte Carlo generator with the MC09, Perugia0 and DW tunes, PHOJET and HERWIG+JIMMY. The Monte Carlo generators reproduce the general features of the data, but fail to describe the detailed behaviour, as can be seen in the figures. The MC09 and Perugia0 PYTHIA tunes are closest to the data. The PHOJET generator significantly underestimates the particle densities, while the PYTHIA DW and HERWIG overestimate the data at $\Delta\phi \simeq 0$. The data are seen to have a large discriminating power and are thus useful to constrain the parameters of Monte Carlo generators.

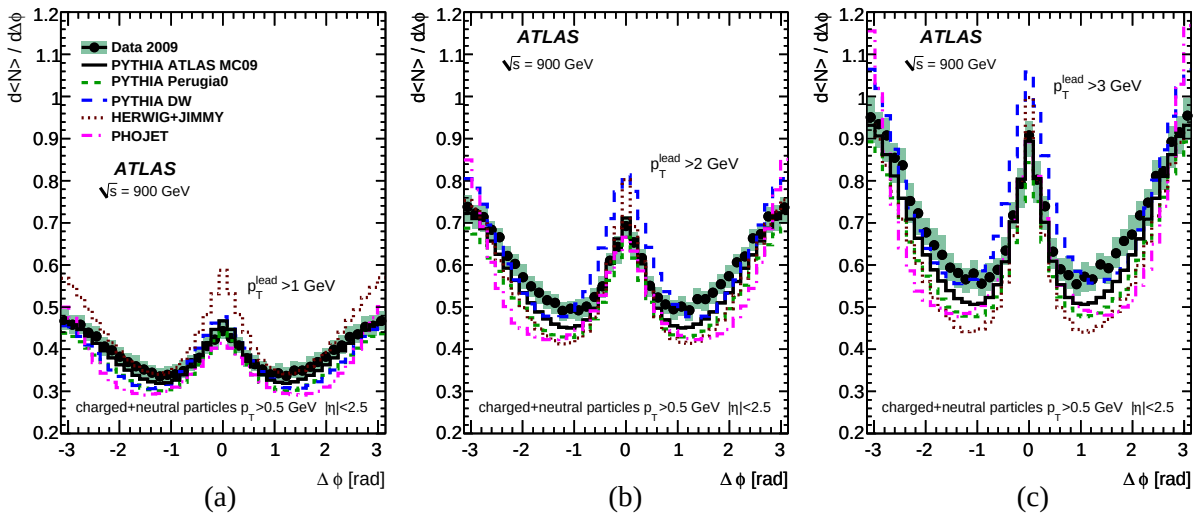

Figure 8: The average number of particles per unit of pseudorapidity as a function of the azimuthal separation between the leading particle and other particles in inelastic pp collisions at $\sqrt{s} = 900$ GeV. The shaded band shows the statistical and systematic uncertainties added in quadrature. The densities are shown for (a) $p_{\mathrm{T}}^{\mathrm{lead}} > 1$ GeV, (b) $p_{\mathrm{T}}^{\mathrm{lead}} > 2$ GeV and (c) $p_{\mathrm{T}}^{\mathrm{lead}} > 3$ GeV.

Figure 10 shows the mean number of particles per event per unit interval in η and ϕ as defined in Sect. 6. The density was calculated in the transverse region illustrated in Fig. 1, as a function of $p_{\mathrm{T}}^{\mathrm{lead}}$. None of the Monte Carlo predictions describe the data well. The DW tune is the most similar to the observed data. As is seen in the $\Delta\phi$ distribution, the PHOJET simulation lacks a hard component for $\sqrt{s} = 7$ TeV. The particle density increases almost by a factor of two, going from $\sqrt{s} = 900$ GeV to $\sqrt{s} = 7$ TeV at a similar $p_{\mathrm{T}}^{\mathrm{lead}}$, which is comparable to what is seen in all Monte Carlo generators.

Figure 11 shows the mean scalar p_{T} sum for stable particles in the transverse region as a function of $p_{\mathrm{T}}^{\mathrm{lead}}$. As for the particle densities, the mean transverse-momentum sum is measured per unit interval in η and ϕ (see Sect. 6). Again, the Monte Carlo predictions do not fully describe the data. The largest discrepancy with the data is found for the PHOJET generator.

9 Conclusions

Particle densities sensitive to the underlying event in pp collisions at centre-of-mass energies of 900 GeV and 7 TeV are presented. This is the first such analysis completely based on calorimetric measure-

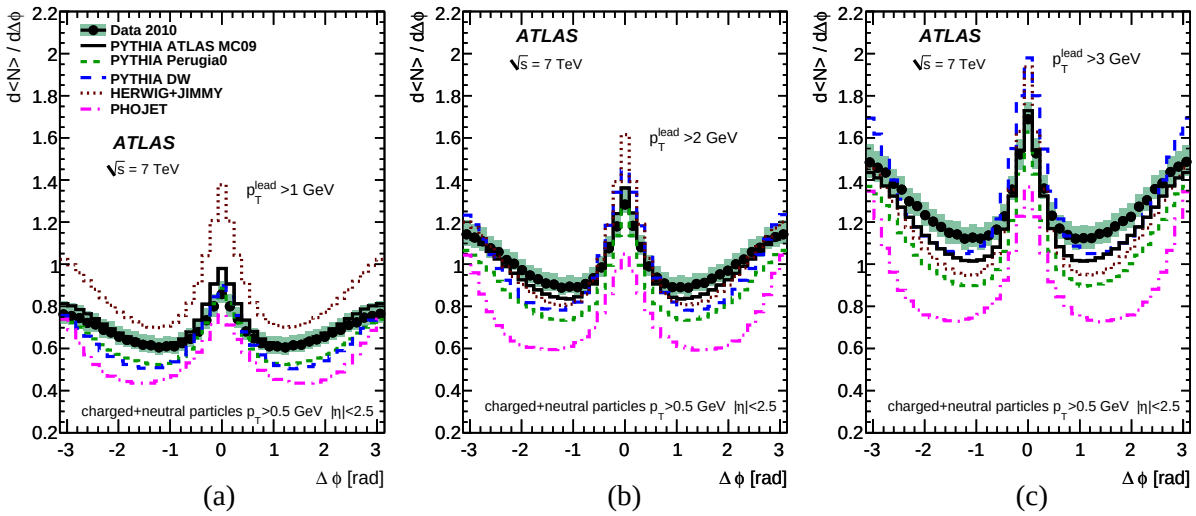

Figure 9: The average number of particles per unit of pseudorapidity as a function of the azimuthal separation between the leading particle and other particles in inelastic pp collisions at $\sqrt{s} = 7$ TeV. The shaded band shows the statistical and systematic uncertainties added in quadrature. The densities are shown for (a) $p_{\mathrm{T}}^{\mathrm{lead}} > 1$ GeV, (b) $p_{\mathrm{T}}^{\mathrm{lead}} > 2$ GeV and (c) $p_{\mathrm{T}}^{\mathrm{lead}} > 3$ GeV.

ment of three-dimensional energy depositions, which is made possible by the fine granularity of the ATLAS calorimeter with transverse and longitudinal samplings.

The particle densities were studied and compared with several Monte Carlo generators tuned to pre-LHC data. None of the Monte Carlo generators describe the measurements well. In particular, the Monte Carlo predictions have discrepancies with the data for the particle density as a function of the azimuthal angle between the leading particle and any other particle in an event. The Monte Carlo generators typically predict a lower particle density in the transverse region ($|\Delta\phi| \simeq \pi/2$), while in the toward region ($\Delta\phi \simeq 0$), the PYTHIA DW and HERWIG+JIMMY generators both overestimate the densities. PHOJET significantly fails for the $\sqrt{s} = 7$ TeV data. For the particle densities as a function of $p_{\mathrm{T}}^{\mathrm{lead}}$, all the Monte Carlo generators also fail to describe the data, predicting lower than observed particle activity in the transverse region. A similar conclusion holds for the total transverse momentum of particles in the transverse region.

The particle densities measured using topological clusters are higher than the charged-particle densities measured using tracks [4]. This is expected from the neutral-particle contribution. The discrepancies between the data and Monte Carlo generators agree with those observed for charged particles [4]. These measurements have systematic uncertainties independent to the track-based studies and provide additional information which may be used to improve the Monte Carlo description of the complete final state produced in pp collisions.

Acknowledgements

We wish to thank CERN for the efficient commissioning and operation of the LHC during this initial high-energy data-taking period as well as the support staff from our institutions without whom ATLAS could not be operated efficiently.

We acknowledge the support of ANPCyT, Argentina; YerPhI, Armenia; ARC, Australia; BMWF, Austria; ANAS, Azerbaijan; SSTC, Belarus; CNPq and FAPESP, Brazil; NSERC, NRC and CFI, Canada;

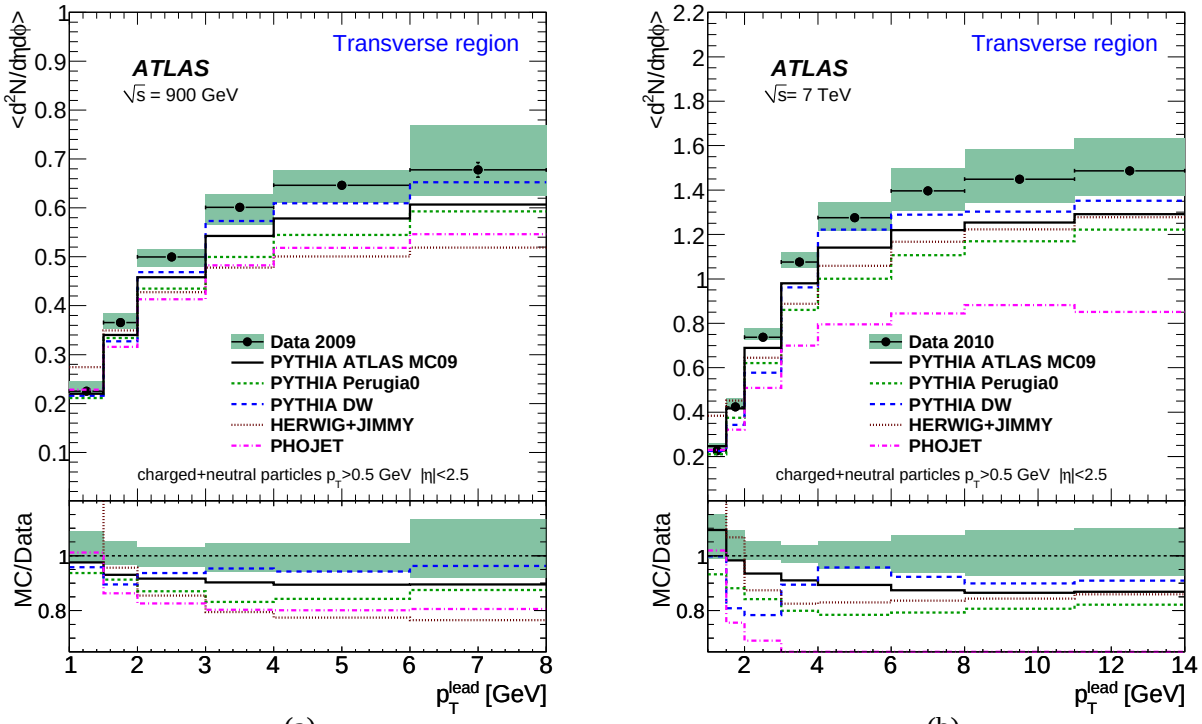

(a) (b)

Figure 10: The average number of stable particles per event per unit interval in η–ϕ, as a function of $p_{\mathrm{T}}^{\mathrm{lead}}$, for the transverse region indicated in Fig. 1. The results are shown for (a) $\sqrt{s} = 900$ GeV and (b) for $\sqrt{s} = 7$ TeV pp collisions. The shaded band shows the statistical and systematic uncertainties added in quadrature.

CERN; CONICYT, Chile; CAS, MOST and NSFC, China; COLCIENCIAS, Colombia; MSMT CR, MPO CR and VSC CR, Czech Republic; DNRF, DNSRC and Lundbeck Foundation, Denmark; ARTEMIS, European Union; IN2P3-CNRS, CEA-DSM/IRFU, France; GNAS, Georgia; BMBF, DFG, HGF, MPG and AvH Foundation, Germany; GSRT, Greece; ISF, MINERVA, GIF, DIP and Benoziyo Center, Israel; INFN, Italy; MEXT and JSPS, Japan; CNRST, Morocco; FOM and NWO, Netherlands; RCN, Norway; MNiSW, Poland; GRICES and FCT, Portugal; MERYS (MECTS), Romania; MES of Russia and ROSATOM, Russian Federation; JINR; MSTD, Serbia; MSSR, Slovakia; ARRS and MVZT, Slovenia; DST/NRF, South Africa; MICINN, Spain; SRC and Wallenberg Foundation, Sweden; SER, SNSF and Cantons of Bern and Geneva, Switzerland; NSC, Taiwan; TAEK, Turkey; STFC, the Royal Society and Leverhulme Trust, United Kingdom; DOE and NSF, United States of America.

The crucial computing support from all WLCG partners is acknowledged gratefully, in particular from CERN and the ATLAS Tier-1 facilities at TRIUMF (Canada), NDGF (Denmark, Norway, Sweden), CC-IN2P3 (France), KIT/GridKA (Germany), INFN-CNAF (Italy), NL-T1 (Netherlands), PIC (Spain), ASGC (Taiwan), RAL (UK) and BNL (USA) and in the Tier-2 facilities worldwide.

References

[1] R. Field, *Min-bias and the underlying event in Run 2 at CDF*, Acta Phys. Pol. **B 36** (2005) 167.

[2] The CDF Collaboration, T. Aaltonen et al., *Underlying event in hard interactions at the Fermilab Tevatron $p\bar{p}$ collider*, Phys. Rev. D **70** (2004) 072002.

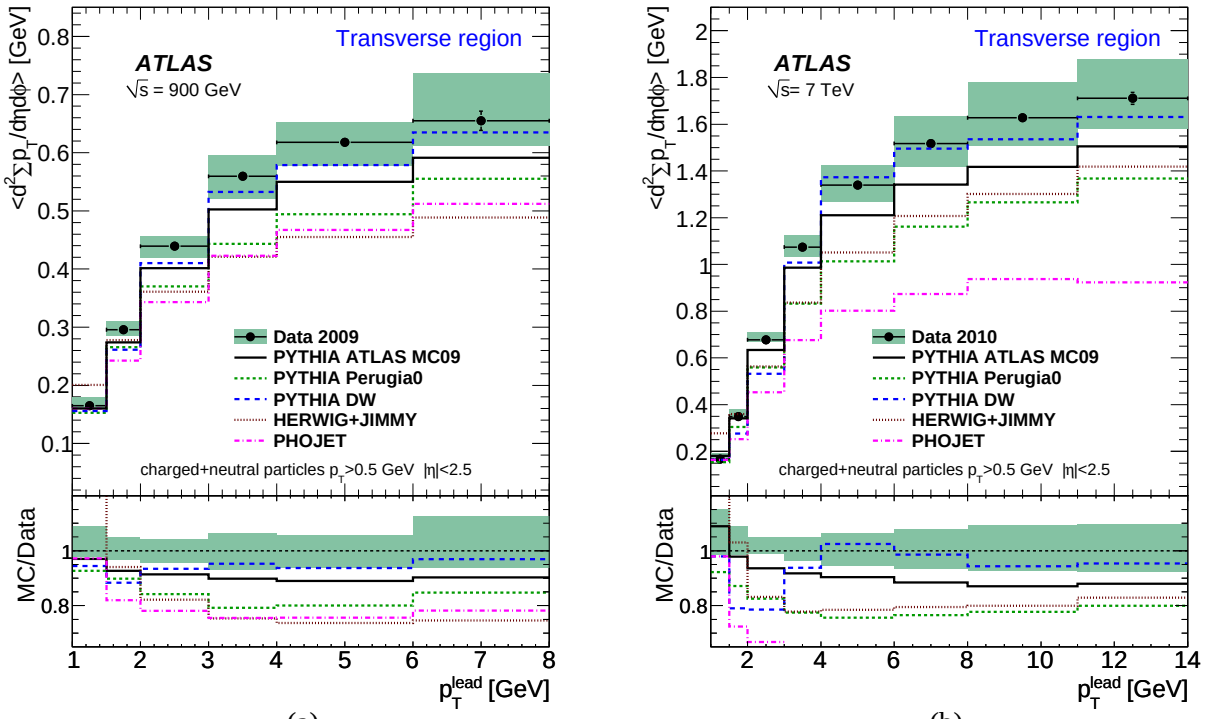

(a) (b)

Figure 11: The average scalar p_{T} sum for stable particles per unit area in η–ϕ in the transverse region as a function of $p_{\mathrm{T}}^{\mathrm{lead}}$ for (a) $\sqrt{s} = 900$ GeV and (b) $\sqrt{s} = 7$ TeV data. The shaded band shows the statistical and systematic uncertainties added in quadrature.

The CDF Collaboration, T. Aaltonen et al., *Studying the Underlying Event in Drell-Yan and High Transverse Momentum Jet Production at the Tevatron*, Phys. Rev. **D 82** (2010) 034001.

[3] The CMS Collaboration, V. Khachatryan et al., *First Measurement of the Underlying Event Activity at the LHC with* $\sqrt{s} = 0.9$ *TeV*, Eur. Phys. J **C 70** (2010) 555.

[4] The ATLAS Collaboration, *Measurement of underlying event characteristics using charged particles in pp collisions at* $\sqrt{s} = 900$*GeV and 7 TeV with the ATLAS detector*, Phys. Rev. D (in press) (2010) , `arXiv:1012.0791 [hep-ex]`.

[5] The ATLAS Collaboration, *The ATLAS Experiment at the CERN Large Hadron Collider*, JINST **3** (2008) S08003.

[6] The ATLAS Collaboration, *Calorimeter Clustering Algorithms: Description and Performance*, ATLAS-LARG-PUB-2008-002 (2008) .

[7] The ATLAS Collaboration, *Local Hadronic Calibration*, ATLAS-LARG-PUB-2009-001 (2008) .

[8] B. Andrieu et al., *Results from pion calibration runs for the H1 liquid argon calorimeter and comparisons with simulation*, Nucl. Instrum. Meth. **A 386** (1997) 348.

E. Abat, E. Arik, S. Cetin, J. Abdallah, M. Bosman, et al., *Study of the response of the ATLAS central calorimeter to pions of energies from 3 to 9 GeV*, Nucl. Instrum. Meth. **A 607** (2009) 372.

P. Adragna, C. Alexa, K. Anderson, A. Antonaki, A. Arabidze, et al., *Testbeam studies of production modules of the ATLAS tile calorimeter*, Nucl. Instrum. Meth. **A 606** (2009) 362.

M. Aharrouche, C. Adam-Bourdarios, M. Aleksa, D. Banfi, D. Benchekroun, et al., *Measurement of the response of the ATLAS liquid argon barrel calorimeter to electrons at the 2004 combined test-beam*, Nucl. Instrum. Meth. **A 614** (2010) 400.

[9] The ATLAS Collaboration, *Readiness of the ATLAS Liquid Argon Calorimeter for LHC Collisions*, Eur. Phys. J. **C 70** (2010) 723.

The ATLAS Collaboration, *Readiness of the ATLAS Tile Calorimeter for LHC collisions*, Eur. Phys. J. **C 70** (2010) 1193.

[10] The ATLAS Collaboration, *Charged-particle multiplicities in pp interactions at* $\sqrt{s} = 900$ *GeV measured with the ATLAS detector at the LHC*, Phys. Lett. **B 688** (2010) 21.

[11] The ATLAS Collaboration, *Performance of primary vertex reconstruction in proton-proton collisions at* $\sqrt{s}$ *=7 TeV in the ATLAS experiment*, ATLAS-CONF-2010-069 (2010) .

[12] T. Sjostrand, S. Mrenna, and P. Z. Skands, *PYTHIA 6.4 Physics and Manual*, JHEP **05** (2006) 026.

[13] The ATLAS Collaboration, *ATLAS Monte Carlo tunes for MC09*, ATLAS-PHYS-PUB-2010-002 (2010) .

[14] A. Sherstnev and R. S. Thorne, *Parton Distributions for LO Generators*, Eur. Phys. J. **C 55** (2008) 553.

[15] B. Andersson, G. Gustafson, G. Ingelman, and T. Sjostrand, *Parton Fragmentation and String Dynamics*, Phys. Rept. **97** (1983) 31.

[16] The CDF Collaboration, F. Abe et al., *Transverse momentum distributions of charged particles produced in* $\bar{p}p$ *interactions at* $\sqrt{s} = 630$ *GeV and 1800 GeV*, Phys. Rev. Lett. **61** (1988) 1819.

[17] P. Z. Skands, *The Perugia Tunes*, `arXiv:0905.3418 [hep-ph]`. Presented at Multi-Parton Interaction Workshop, Perugia, Italy, 28-31 Oct 2008. Published in Perugia 2008, Multiple Partonic Interactions at the LHC (MPI08) p.284.

[18] R. Field, *MinBias and the Underlying Event at the Tevatron and the LHC, A talk presented at the Fermilab mc tuning workshop*, tech. rep., FERMILAB, 2002.

[19] R. Engel and J. Ranft, *Color singlet exchange between jets and the PHOJET Monte Carlo*, Nucl. Phys. Proc. Suppl. **A 75** (1999) 272.

[20] G. Corcella et al., *HERWIG 6.5: an event generator for Hadron Emission Reactions With Interfering Gluons (including supersymmetric processes)*, JHEP **01** (2001) 010.

[21] G. Corcella et al., *HERWIG 6.5 release note*, `arXiv:hep-ph/0210213`.

[22] J. M. Butterworth, J. R. Forshaw, and M. H. Seymour, *Multiparton interactions in photoproduction at HERA*, Z. Phys. **C 72** (1996) 637.

[23] The ATLAS Collaboration, *The ATLAS simulation software*, Nucl. Phys. Proc. Suppl. **197** (2009) 254.

[24] S. Agostinelli et al., GEANT4*–a simulation toolkit*, Nucl. Instr. Meth. **A 506** (2003) no. 3, 250.

[25] The ATLAS Collaboration, *ATLAS Calorimeter Response to Single Isolated Hadrons and Estimation of the Calorimeter Jet Scale Uncertainty*, ATLAS-CONF-2010-052 (2010) .

[26] The ATLAS Collaboration, *Response of the ATLAS calorimeters to single isolated hadrons produced in proton proton collisions at a center of mass energy of $\sqrt{s}$ = 900 GeV*, ATLAS-CONF-2010-017 (2010) .

[27] The ATLAS Collaboration, *Properties of Jets and Inputs to Jet Reconstruction and Calibration with the ATLAS Detector Using Proton-Proton Collisions at $\sqrt{s} = 7$ TeV*, ATLAS-CONF-2010-053 (2010) .

[28] M. Cacciari, G. P. Salam, and G. Soyez, *The anti-kT jet clustering algorithm*, JHEP **04** (2008) 063.

[29] UA1 Collaboration, C. Albajar et al., *Production of low transverse energy clusters in collisions at $\sqrt{s}$=0.2-0.9 TeV and their interpretation in terms of QCD jets*, Nucl. Phys. **B 309** (1988) no. 3, 405.

The ATLAS Collaboration

Argentina
Buenos Aires
M.L. Gonzalez Silva, G. Otero y Garzon, R. Piegaia, G. Romeo

La Plata
X.S. Anduaga, M.T. Dova, F. Monticelli, M.F. Tripiana

Armenia
Yerevan
V. Grabski, H. Hakobyan

Australia
Melbourne
E.L. Barberio, W. Davey, N. Davidson, C.U. Felzmann, S.I. Kazi, A. Limosani, G.F. Moorhead, A. Phan, M.E. Sevior, Q.T. Shao, G.N. Taylor, M.J. White

Sydney
J.S.H. Lee, N. Patel, A.F. Saavedra, K.E. Varvell, A.T. Waugh, B. Yabsley

Austria
FHWN
E. Griesmayer

Innsbruck
B. Epp, P. Jussel, E. Kneringer, D. Kuhn, G. Rudolph

Azerbaijan
Baku
O. Abdinov, M. Aliyev, F. Khalil-zada, S. Rzaeva

Brazil
Rio de Janeiro UF
L.P. Caloba, A.S. Cerqueira, R. Coura Torres, A. Da Rocha Gesualdi Mello, P.V.M. Da Silva, M.A.B. do Vale, C. Maidantchik, F. Marroquim, A.A. Nepomuceno, M. Perantoni, J.M. Seixas

USP
M. Donadelli, M.A.L. Leite

Canada
Alberta
S. Bahinipati, N.J. Buchanan, K. Chan, L. Chen, D.M. Gingrich, M.S. Kim, S. Liu, J. Lu, R.W. Moore, J.L. Pinfold, N. Soni, S. Subramania

Carleton
J.P. Archambault, C.D. Cojocaru, D. Gillberg, L. Heelan, M. Khakzad, C. Liu, T.G. McCarthy, F.G. Oakham, K. Randrianarivony, R. Ueno, M.G. Vincter, K. Whalen

McGill
B. Chapleau, F. Corriveau, M. Dobbs, M-A. Dufour, H. Guler, M. Klemetti, C.T. Potter, S.H. Robertson, C. Santamarina Rios, M. Schram, B. Vachon, A. Warburton

Montreal

G. Azuelos, P. Banerjee, J. Bouchami, M. Davies, J. Ferland, A. Gutierrez, C. Lebel, C. Leroy, J.A. Macana Goia, J.P. Martin, R. Mehdiyev, O. Scallon

Regina
K. Benslama, X. Ju, Y. Ming, E.O. Ortega

Simon Fraser Burnaby
E. Dawe, J. Godfrey, J.R. Komaragiri, D.C. O'Neil, M. Petteni, D. Schouten, B. Stelzer, M. Trottier-McDonald, M.C. Vetterli

Toronto
D.C. Bailey, T. Bain, B. Beare, B. Brelier, S.L. Cheung, P.O. Deviveiros, S. Dhaliwal, T. Farooque, B. Fatholahzadeh, A. Gibson, B. Guo, E. Jankowski, P. Krieger, C. Le Maner, F.K. Martens, R.S. Orr, R. Rezvani, G.A. Rosenbaum, P. Sandhu, P. Savard, P. Sinervo, T. Spreitzer, D. Tardif, R.J. Teuscher, P.D. Thompson, W. Trischuk

TRIUMF
A. Canepa, B. Caron, S.V. Chekulaev, D. Fortin, M.J. Losty, I.M. Nugent, C.J. Oram, O. Stelzer-Chilton, R. Tafirout, I.M. Trigger

Vancouver UBC
D. Axen, C. Gay, C.W. Loh, W.J. Mills, A. Muir, S. Swedish, S. Viel

Victoria
A. Astbury, Sw. Banerjee, V. Bansal, F. Berghaus, L. Courneyea, M. Fincke-Keeler, R. Keeler, R. Kowalewski, M. Lefebvre, J-R. Lessard, R.A. McPherson, M. Plamondon, R. Sobie

York
W. Taylor

Chile
Santiago
M.A. Diaz, B. Panes, F. Quinonez, D. Romero Maltrana, P. Urrejola

Valparaiso
W.K. Brooks, S. Kuleshov, A. Oyarzun, R. Pezoa, F. Prokoshin

China
Beijing
Y. Bai, S. Cheng, H. Han, S. Jin, F. Lu, Q. Ouyang, L.Y. Shan, G. Tong, Y. Xie, G. Xu, Y. Yang, L. Yuan, S. Zheng

Hefei
L. Han, Y. Jiang, G. Jin, S. Li, M. Liu, Y. Liu, Y. Wu, C. Xu, D. Zhang, Z. Zhao

Nanjing
S. Chen, T. Chen, J. Ping, J. Yu

Shandong
C. Feng, P. Ge, M. He, J. Miao, J. Wang, Z. Zhan, X. Zhang, C.G. Zhu

Colombia
UAN Bogota
M. Losada, K.F. Loureiro, L. Mendoza Navas, G. Navarro, D. Rodriguez

Czech Republic

Olomouc
P. Hamal, A. Kocnar

Prague AS
J. Chudoba, P. Gallus, J. Gunther, I. Hruska, V. Juranek, O. Kepka, A. Kupco, V. Kus, O. Kvasnicka, L. Lipinsky, M. Lokajicek, M. Marcisovsky, M. Mikestikova, M. Myska, S. Nemecek, M. Panuskova, P. Ruzicka, J. Schovancova, P. Sicho, P. Staroba, M. Tasevsky, T. Tic, J. Valenta, V. Vrba

Prague CU
T. Davidek, J. Dolejsi, Z. Dolezal, Z. Drasal, P. Kodys, R. Leitner, J. Novakova, M. Rybar, M. Spousta, P. Strachota, M. Suk, T. Sykora, P. Tas, S. Valkar, V. Vorobel, I. Wilhelm

Prague TU
K. Augsten, T. Holy, T. Horazdovsky, Z. Hubacek, J. Jakubek, Z. Kohout, V. Kral, F. Krejci, S. Pospisil, V. Simak, T. Slavicek, K. Smolek, J. Sodomka, M. Solar, J. Solc, V. Sopko, B. Sopko, I. Stekl, D. Turecek, V. Vacek, M. Vlasak, P. Vokac

Denmark
Copenhagen NBI
N. Boelaert, M. Dam, C. Driouichi, K. Facius, J.R. Hansen, J.B. Hansen, J.D. Hansen, P.H. Hansen, S. Heisterkamp, S. Jakobsen, P. Jež, M.D. Joergensen, P. Kadlecik, E.B. Klinkby, J. Lundquist, R. Mackeprang, S. Mehlhase, T.C. Petersen, B. Rensch, M. Simonyan, S. Xella

France
Annecy LAPP
L. Aperio Bella, B. Aubert, M. Aurousseau, N. Berger, J. Colas, L. Di Ciaccio, T.K.O. Doan, M. El Kacimi, S. Elles, P. Ghez, M. Gouanère, C. Goy, T. Guillemin, L. Helary, T. Hryn'ova, P. Iengo, G. Ionescu, A. Jeremie, S. Jézéquel, M. Kataoka, J. Labbe, R. Lafaye, N. Massol, P. Perrodo, H. Przysiezniak, G. Sauvage, T. Todorov, D. Tsionou, I. Wingerter-Seez, R. Zitoun, Y. Zolnierowski

Clermont - Ferrand
E. Busato, D. Calvet, S. Calvet, R. Camacho Toro, D. Cinca, R. Febbraro, N. Ghodbane, P.L.Y. Gris, C. Guicheney, D. Pallin, F. Podlyski, C. Santoni, L.P. Says, F. Vazeille, S. Viret

Grenoble LPSC
S. Albrand, M-L. Andrieux, B. Clement, J. Collot, S. Crépé-Renaudin, P. de Saintignon, P.A. Delsart, J. Donini, D. Dzahini, J-Y. Hostachy, E. Laisne, F. Ledroit-Guillon, A. Lleres, A. Lucotte, F. Malek, Ph. Martin, F. Polci, J. Stark, X. Sun, B. Trocmé

LPNHE-Paris
T. Beau, S. Bordoni, G. Calderini, A. Camard, P. Cavalleri, E. Chareyre, S. De Cecco, F. Derue, D. Imbault, M.W. Krasny, D. Lacour, B. Laforge, S. Laplace, O. Le Dortz, J. Lellouch, G. Marchiori, I. Nikolic-Audit, J. Ocariz, M. Ridel, L. Roos, Ph. Schwemling, T. Theveneaux-Pelzer, S. Trincaz-Duvoid, T.N. Trinh, F. Vannucci

Marseille CPPM
S. Aoun, C. Bee, C. Benchouk, K. Bernardet, N. Bousson, J.C. Clemens, Y. Coadou, P. Delpierre, F. Djama, F. Etienne, L. Feligioni, F. Henry-Couannier, D. Hoffmann, F. Hubaut, E.B.F.G. Knoops, M. Kuna, E. Le Guirriec, J. Levêque, B. Li, E. Monnier, J. Odier, E. Petit, P. Pralavorio, Z. Qian, A. Rozanov, M. Talby, N. Tannoury, S. Tisserant, J. Toth, F. Touchard, L. Vacavant

Orsay LAL
H. Abreu, C. Arnault, E. Auge, P. Barrillon, M. Benoit, S. Binet, J.-B. Blanchard, C. Bourdarios, D. Breton, C. Collard, C. De La Taille, J.B. De Vivie De Regie, S. Diglio, L. Duflot, M. Escalier,

A.C. Falou, L. Fayard, D. Fournier, J.-F. Grivaz, M. Heller, S. Henrot-Versille, J. Hrivnac, L. Iconomidou-Fayard, J. Idarraga, M. Kado, A. Lounis, N. Makovec, P. Matricon, Y. Nakahama, F. Niedercorn, L. Poggioli, P. Puzo, A. Renaud, D. Rousseau, X. Ruan, G. Rybkin, J.B. Sauvan, J. Schaarschmidt, A.C. Schaffer, L. Serin, S. Simion, R. Tanaka, J.J. Veillet, I. Vukotic, F. Wicek, D. Zerwas, Z. Zhang

Saclay CEA
H. Bachacou, F. Bauer, N. Besson, M. Boonekamp, L. Chevalier, F. Chevallier, J. Ernwein, A.I. Etienvre, A. Formica, L. Gauthier, P.F. Giraud, C. Guyot, S. Hassani, W. Kozanecki, E. Lancon, J.F. Laporte, E. Le Menedeu, M. Legendre, B. Lenzi, B. Mansoulie, J-P. Meyer, N. Morange, R. Nicolaidou, A. Ouraou, D.M. Pomarede, B. Resende, C.R. Royon, Ph. Schune, J. Schwindling, O. Simard, M. Virchaux

FR-CCIN2P3 Tier-1
C. Biscarat, E. Cogneras, G. Rahal

Georgia
Tbilisi IP
L. Chikovani, E.G. Tskhadadze

Tbilisi SU
T. Djobava, J. Khubua, E. Magradze, G. Mchedlidze, M. Mosidze

Germany
Berlin HU
M. Aliev, G. Brandt, F.M. Giorgi, S. Grancagnolo, R. Herrberg, O. Kind, H. Kolanoski, R. Kwee, H. Lacker, M. Leyton, T. Lohse, R. Mandrysch, A. Nikiforov, Y. Rodriguez Garcia, H. Schulz, A. Sidoti, M. zur Nedden

Bonn
M. Alhroob, C.F. Anders, D. Arutinov, M. Backhaus, M. Barbero, D. Bartsch, I. Brock, J. Cammin, M. Cristinziani, K. Desch, J. Dingfelder, P. Fischer , G. Gaycken, Ch. Geich-Gimbel, L. Gonella, M. Havranek, S. Hillert, F. Huegging, T. Ince, M. Janus, G. Khoriauli, P. Koevesarki, T. Kokott, V.V. Kostyukhin, J. Kroseberg, H. Krüger, A. Kruth, C. Lapoire, M. Lehmacher, T. Loddenkoetter, M. Mathes, M. Mazur, S. Meuser, N. Möser, K. Mueller, G. Nanava, T. Nattermann, A.-E. Nuncio-Quiroz, G. Nunes Hanninger, I. Peric, T. Poghosyan, S. Psoroulas, B. Radics, I. Rottländer, O. Runolfsson, K. Schmieden, M. Schmitz, J.W. Schumacher, J.A. Stillings, T. Stockmanns, J. Therhaag, J. Treis, J.-W. Tsung, K. Uchida, M. Uhlenbrock, N. Vlasov, A. Vogel, E. von Toerne, N. Wermes, P. Wienemann, C. Zendler, R. Zimmermann, S. Zimmermann

DESY
P. Bechtle, E. Bergeaas Kuutmann, M. Boehler, W. Ehrenfeld, V. Ferrara, G. Fischer, A. Glazov, M. Goebel, L.S. Gomez Fajardo, B. Gosdzik, I.M. Gregor, K.H. Hiller, I. Hristova , U. Husemann, M. Jimenez Belenguer, S. Johnert, M. Karnevskiy, J. Katzy, T. Kono, C. Lange, E. Lobodzinska, D. Ludwig, S. Mättig, M. Medinnis, L. Mijović, K. Mönig, T. Naumann, M. Nožička, T. Perez Cavalcanti, D. Petschull, S.M. Piec, R. Placakyte, Z. Qin, I. Rubinskiy, H.J. Stelzer, M. Terwort, P. Vankov, M. Viti, M.A. Wildt, H. Zhu

Dortmund
M. Bunse, D. Dobos, C. Gössling, F. Hirsch, J. Klaiber-Lodewigs, R. Klingenberg, O. Krasel, M. Maß, D. Muenstermann, S. Rajek, I. Reisinger, J. Walbersloh, J. Weber, R. Wunstorf

Dresden

T. Göpfert, D. Kar, M. Kobel, K. Leonhardt, A. Ludwig, W.F. Mader, X. Prudent, R. Schwierz, F. Seifert, P. Steinbach, A. Straessner, A. Vest

Freiburg

G. Aad, F. Ahles, M. Beckingham, R. Bernhard, U. Bitenc, R. Bruneliere, S. Caron, C. Carpentieri, A. Christov, A. Dahlhoff, J. Dietrich, S. Eckert, M. Fehling-Kaschek, M. Flechl, J. Glatzer, J. Hartert, M. Heldmann, G. Herten, S. Horner, K. Jakobs, C. Ketterer, S. König, M. Kollefrath, A.I. Kononov, S. Kuehn, S. Lai, U. Landgraf, K. Lohwasser, I. Ludwig, J. Ludwig, D. Lumb, K. Mahboubi, J. Meinhardt, W. Mohr, H. Nilsen, U. Parzefall, X. Portell Bueso, M. Rammensee, K. Runge, Z. Rurikova, E. Schmidt, M. Schumacher, F. Siegert, K. Stoerig, J.E. Sundermann, K.K. Temming, S. Thoma, J. Tobias, V. Tsiskaridze, M. Venturi, I. Vivarelli, H. von Radziewski, M. Warsinsky, C. Weiser, M. Werner, L.A.M. Wiik, S. Winkelmann, S. Xie, S. Zimmermann

Giessen

A. Astvatsatourov, M. Düren, H. Stenzel

Goettingen

C. Ay, U. Blumenschein, O. Brandt, J. Erdmann, D. Evangelakou, J. Grosse-Knetter, S. Guindon, J. Haller, A. Henrichs, C. Hensel, M. Keil, A. Knue, F. Kohn, N. Krieger, K. Kroeninger, A. Mann, J. Meyer, J. Morel, A. Quadt, A. Roe, E. Shabalina, M. Uhrmacher, P. Weber, J. Weingarten

Heidelberg KIP

V. Andrei, J.T. Childers, T.A. Dietzsch, F. Föhlisch, C. Geweniger, P. Hanke, M. Henke, A. Khomich, E.-E. Kluge, V. Lendermann, K. Meier, F. Mueller, S. Poddar, V. Scharf, H.-C. Schultz-Coulon, R. Stamen, M. Wessels

Heidelberg PI

V. Radescu, S. Schaetzel, A. Schöning

Heidelberg ZITI

A. Kugel, R. Maenner, N. Schroer

Mainz

M. Aharrouche, O. Arnaez, M. Bendel, W. Blum, V. Büscher, S. Eckweiler, K. Edmonds, F. Ellinghaus, E. Ertel, F. Fiedler, J. Fleckner, C. Goeringer, C. Handel, M. Hohlfeld, W. Ji, G. Kawamura, K. Kleinknecht, S. Koenig, L. Köpke, M. Lungwitz, L. Masetti, C. Meyer, D. Moreno, A. Neusiedl, S. Rieke, H.G. Sander, U. Schäfer, C. Schmitt, C. Schroeder, G. Siragusa, S. Tapprogge, T. Vu Anh

Munich LMU

S. Adomeit, O. Biebel, P. Calfayan, J. de Graat, M. Deile, G. Duckeck, J. Ebke, J. Elmsheuser, A. Engl, C. Galea, M.H. Genest, R. Hertenberger, J. Kennedy, C. Kummer, F. Legger, M. Lichtnecker, R. Mameghani, T.A. Müller, T. Nunnemann, F. Rauscher, P. Reznicek, B. Ruckert, M.P. Sanders, D. Schaile, J. Schieck, C. Serfon, A. Staude, R. Walker, J.Z. Will, X. Zhuang

Munich MPI

M. Aderholz, T. Barillari, M. Beimforde, S. Bethke, D. Capriotti, G. Cortiana, D. Dannheim, H. Dietl, J. Dubbert, T. Ehrich, M.J. Flowerdew, P. Giovannini, T. Göttfert, M. Groh, P. Haefner, D. Hauff, T. Hott, A. Jantsch, S. Kaiser, A.E. Kiryunin, S. Kluth, O. Kortner, S. Kortner, S. Kotov, H. Kroha, G. Lutz, A. Macchiolo, A. Manz, S. Menke, S. Mohrdieck-Möck, H.G. Moser, R. Nisius, H. Oberlack, G.E. Pospelov, I.N. Potrap, E. Rauter, R. Richter, D. Salihagic, P. Schacht, R. Seuster, S. Stonjek, C. Valderanis, H. von der Schmitt, J. von Loeben, P. Weigell, V. Zhuravlov

Siegen

P. Buchholz, H. Czirr, I. Fleck, B. Gaur, K. Grybel, M. Holder, I. Ibragimov, M. Rammes, V. Sipica, T. Stahl, W. Walkowiak, M. Ziolkowski

Wuerzburg
P. Fleischmann, J. Meyer, A. Redelbach, R. Ströhmer, T. Trefzger

Wuppertal
M. Barisonzi, K.H. Becks, J. Boek, H.M. Braun, J. Dopke, J. Drees, S. Fleischmann, T. Flick, P. Gerlach, K.W. Glitza, G. Gorfine, C. Grah, K. Hamacher, T. Harenberg, T. Henß, D. Hirschbuehl, M. Imhaeuser, S. Kalinin, S. Kersten, A. Kootz, T. Kuhl, T. Lenz, G. Lenzen, P. Mättig, M. Mechtel, M. Sandhoff, S. Sandvoss, G. Sartisohn, J. Schultes, A. Siebel, P. Sturm, J. Thadome, T.T. Voss, W. Wagner, H. Wahlen, D. Wicke, C. Zeitnitz

Greece
Athens
A. Antonaki, D. Fassouliotis, V. Giakoumopoulou, N. Giokaris, P. Ioannou, C. Kourkoumelis, A. Manousakis-Katsikakis, G. Tzanakos, C. Vellidis

Athens NTU
T. Alexopoulos, R. Avramidou, M. Dris, A. Filippas, M. Fokitis, E.N. Gazis, G. Iakovidis, E. Katsoufis, S. Leontsinis, S. Maltezos, E. Mountricha, E. Panagiotopoulou, Th.D. Papadopoulou, P. Savva , G. Tsipolitis, S. Vlachos, L. Xaplanteris

Thessaloniki
D. Iliadis, K. Kordas, V. Kouskoura, I. Nomidis, A. Petridis, C. Petridou, D. Sampsonidis

Israel
Technion Haifa
S. Behar Harpaz, S. Ben Ami, S. Bressler, A.D. Hershenhorn, E. Kajomovitz, H. Landsman, R. Lifshitz, Y. Rozen, S. Tarem, Y.D. Tennenbaum-Katan, S. Vallecorsa

Tel-Aviv
H. Abramowicz, G. Alexander, N. Amram, G. Bella, O. Benary, Y. Benhammou, E. Brodet, E. Etzion, A. Gershon, J. Ginzburg, N. Guttman, N. Hod, A. Kreisel, Y. Mahalalel, Y. Munwes, Y. Oren, E. Reinherz-Aronis, I. Sadeh, Y. Silver, A. Soffer, N. Taiblum, E. Urkovsky

Weizmann Rehovot
R. Alon, L. Barak, E. Duchovni, T. Frank, O. Gabizon, E. Gross, A. Klier, D. Lellouch, L.J. Levinson, G. Mikenberg, A. Milov, D. Milstein, I. Roth, O. Silbert, V. Smakhtin, O. Vitells

Italy
Bologna
S. Antonelli, L. Bellagamba, A. Bertin, M. Bindi, D. Boscherini, A. Bruni, G. Bruni, M. Bruschi, D. Caforio, C. Ciocca, M. Corradi, S. De Castro, R. Di Sipio, L. Fabbri, B. Giacobbe, P. Giusti, M.K. Jha, I. Massa, A. Mengarelli, S. Monzani, M. Piccinini, A. Polini, L. Rinaldi, C. Sbarra, A. Sbrizzi, N. Semprini-Cesari, R. Spighi, S. Valentinetti, M. Villa, A. Vitale , A. Zoccoli

Cosenza
M. Capua, G. Crosetti, S. Fazio, L. La Rotonda, A. Mastroberardino, G. Morello, D. Salvatore, M. Schioppa, G. Susinno, E. Tassi

Frascati
A. Annovi, M. Antonelli, H. Bilokon, F. Cerutti, M. Curatolo, B. Esposito, M.L. Ferrer, C. Gatti, P. Laurelli, G. Maccarrone, A. Sansoni, M. Testa, E. Vilucchi, M. Wen

Genova

D. Barberis, R. Beccherle, C. Caso, A. Coccaro, T. Cornelissen, S. Cuneo, M. Dameri, G. Darbo, A. Ferretto Parodi, G. Gagliardi, C. Gemme, P. Morettini, M. Olcese, B. Osculati, F. Parodi, L.P. Rossi, C. Schiavi

Lecce
M. Bianco, E. Brambilla, G. Cataldi, A. Cazzato, G. Chiodini, R. Coluccia, R. Crupi, E. Gorini, F. Grancagnolo, A. Guida, R. Perrino, M. Primavera, S. Spagnolo, A. Ventura

Milano
E. Acerbi, M. Aleppo, F. Alessandria, G. Alimonti, A. Andreazza, G. Baccaglioni, G. Battistoni, G. Bellomo, M.I. Besana, F. Broggi, M. Caccia, L. Carminati, D. Cavalli, G. Costa, L. Dell'Asta, M. Fanti, A. Favareto, D. Giugni, I. Koletsou, T. Lari, A. Lazzaro, V.P. Lombardo, L. Mandelli, M. Mazzanti, C. Meroni, S. Montesano, L. Perini, C. Pizio, F. Ragusa, S. Resconi, G. Rivoltella, L. Rossi, M. Sorbi, G.F. Tartarelli, C. Troncon, G. Vegni, G. Volpini

Napoli
A. Aloisio, M.G. Alviggi, V. Canale, L. Capasso, G. Carlino, F. Cevenini, G. Chiefari, F. Conventi, R. de Asmundis, M. Della Pietra, D. della Volpe, A. Doria, R. Giordano, G. Iacobucci, V. Izzo, L. Merola, E. Musto, S. Patricelli, E. Rossi, G. Sekhniaidze

Pavia
M. Bellomo, M. Cambiaghi, C. Conta, R. Ferrari, S. Franchino, M. Fraternali, G. Gaudio, M. Livan, A. Negri, G. Polesello, D.M. Rebuzzi, A. Rimoldi, M. Uslenghi, V. Vercesi

Pisa
F. Bertolucci, M. Cascella, V. Cavasinni, T. Del Prete, A. Dotti, P. Francavilla, V. Giangiobbe, A. Lupi, E. Mazzoni, C. Roda, F. Sarri, Z. Zenonos

Roma I
F. Anulli, G. Artoni, P. Bagnaia, M. Biglietti, C. Bini, S. Borroni, R. Caloi, A. Cavallari, G. Ciapetti, A. D'Orazio, D. De Pedis, A. De Salvo, C. Dionisi, S. Falciano, S. Gentile, S. Giagu, F. Lacava, F. Lo Sterzo, C. Luci, L. Luminari, C. Maiani, F. Marzano, G. Mirabelli, A. Nisati, E. Pasqualucci, E. Petrolo, L. Pontecorvo, M. Rescigno, F. Safai Tehrani, E. Solfaroli Camillocci, F. Spila, P. Valente, R. Vari, S. Veneziano, L. Zanello

Roma II
G. Aielli, P. Camarri, R. Cardarelli, G. Cattani, A. Di Ciaccio, R. Di Nardo, A. Di Simone, B. Liberti, F. Marchese, A. Paoloni, A. Salamon, R. Santonico

Roma Tre
C. Bacci, A. Baroncelli, P. Branchini, F. Ceradini, S. Di Luise, B. Di Micco, A. Farilla, E. Graziani, M. Iodice, D. Orestano, A. Passeri, F. Pastore, F. Petrucci, F. Ruggieri, E. Spiriti, C. Stanescu, A. Tonazzo

Trieste ICTP
B.S. Acharya, K. Suruliz

Udine
D. Cauz, M. Cobal, B. De Lotto, U. De Sanctis, C. Del Papa, M. Pinamonti, K. Shaw

Japan
Hiroshima
T. Ohsugi

Hiroshima IT

Y. Nagasaka

KEK
K. Amako, Y. Arai, Y. Doi, T. Haruyama, Y. Ikegami, M. Ikeno, K. Ishii, M. Ishino, H. Iwasaki, J. Kanzaki, T. Kohriki, T. Kondo, Y. Makida, A. Manabe, S. Mitsui, Y. Morita, K. Murakami, K. Nagano, M. Nozaki, S. Odaka, T.K. Ohska, O. Sasaki, T. Sasaki, Y. Suzuki, S. Tanaka, S. Terada, J. Tojo, K. Tokushuku, S. Tsuno, Y. Unno, M. Yamada, A. Yamamoto, Y. Yasu

Kobe
T. Hayakawa, Y. Homma, R. Ichimiya, A. Ishikawa, K. Kawagoe, M. King, H. Kiyamura, H. Kurashige, T. Matsushita, K. Miyazaki, T. Nishiyama, A. Ochi, S. Okada, C. Omachi, K. Suita, H. Takeda, K. Tani, K. Tokunaga, Y. Yamazaki

Kyoto
N. Sasao

Kyoto UE
R. Takashima

Nagasaki
M. Shimojima, Y. Tanaka

Nagoya
S. Hasegawa, Y. Itoh, T. Ohshima, Y. Okumura, T. Sugimoto, Y. Takahashi, M. Tomoto, J. Wakabayashi

Okayama
I. Nakano

Osaka
K. Hanagaki, M. Hirose, T. Meguro, M. Nomachi, Y. Sugaya

Ritsumeikan
S. Tanaka

Shinshu
Y. Hasegawa, H. Ohshita, T. Takeshita

Tokyo ICEPP
G. Akimoto, S. Asai, Y. Azuma, T. Dohmae, M. Imori, T. Isobe, N. Kanaya, M. Kaneda, Y. Kataoka, T. Kawamoto, K. Kessoku, T. Kobayashi, T. Kubota, T. Mashimo, T. Masubuchi, H. Matsumoto, H. Matsunaga, K. Nakamura, Y. Ninomiya , H. Nomoto, S. Oda, T. Okuyama, H. Sakamoto, J. Tanaka, K. Terashi, I. Ueda, S. Yamamoto, T. Yamamura, T. Yamazaki

Tokyo MU
U. Bratzler, C. Fukunaga

Tokyo Tech
O. Jinnouchi, T. Kanno, M. Kuze

Tsukuba
K. Hara, S.H. Kim, M. Kurata, K. Nagai, F. Ukegawa

Waseda
N. Kimura, K. Yorita

Morocco
Casablanca

D. Benchekroun, A. Chafaq, M. Gouighri, D. Goujdami, A. Hoummada

CNESTEN Rabat

Oujda
J.E. Derkaoui, M. Ouchrif

Rabat
R. Cherkaoui El Moursli, H. Ghazlane

Netherlands
Nijmegen
M. Consonni, N. De Groot, F. Filthaut, P.F. Klok, A.C. König, F. Koetsveld, C.A. Magrath, G. Ordonez, M. Raas, C.J.W.P. Timmermans

Nikhef
S. Bentvelsen, G.J. Bobbink, K. Bos, H. Boterenbrood, E.J. Buis, A.P. Colijn, R. Dankers, C. Daum, P. de Jong, L. De Nooij, A.D. Doxiadis, P. Ferrari, H. Garitaonandia, D.A.A. Geerts, M. Gosselink, F. Hartjes, N.P. Hessey, O. Igonkina, M.S. Kayl, S. Klous, P. Kluit, E. Koffeman, A. Koutsman, H. Lee, F. Linde, G. Luijckx, G. Massaro, J. Mechnich, A. Muijs, I. Mussche, J.P Ottersbach, O. Peters, A. Reichold, M. Rijpstra, N. Ruckstuhl, G. Salamanna, R. Sandstroem, J. Snuverink, D. Ta, M. Tsiakiris, E. Turlay, H. van der Graaf, E. van der Kraaij, R. Van Der Leeuw, E. van der Poel, B. Van Eijk, Z. van Kesteren, I. van Vulpen, W. Verkerke, J.C. Vermeulen, M. Vreeswijk

Norway
Bergen
T. Buanes, T. Burgess, G. Eigen, L.G. Johansen, A. Kastanas, W. Liebig, A. Lipniacka, B. Mohn, O.K. Øye, P.L. Rosendahl, H. Sandaker, T.B. Sjursen, B. Stugu, A. Tonoyan, M. Ugland

Oslo
L. Bugge, T. Buran, D. Cameron, Z. Czyczula, B.K. Gjelsten, E. Lund, F. Ould-Saada, K. Pajchel, Y. Pylypchenko, A.L. Read, O. Røhne, B.H. Samset, S. Stapnes, A. Strandlie, A. Taga

Poland
Cracow AGH-UST
K. Ciba, W. Dabrowski, M. Dwuznik, M. Idzik, K. Jelen, D. Kisielewska, S. Koperny, T.Z. Kowalski, B. Mindur, E. Rulikowska-Zarebska, B. Toczek

Cracow IFJ PAN
E. Banas, J. Blocki, P.A. Bruckman de Renstrom, D. Derendarz, E. Gornicki, Z. Hajduk, W. Iwanski, A. Kaczmarska, K. Korcyl, Pa. Malecki, P. Malecki, A. Olszewski, J. Olszowska, E. Richter-Was, A. Trzupek, M. Turala, M.W. Wolter, B.K. Wosiek, A. Zemla

Portugal
Portugal LIP
A. Amorim, N. Anjos, J. Carvalho, N.F. Castro, P. Conde Muiño, A. Do Valle Wemans, B. Fernandes, M.C.N. Fiolhais, A. Gomes, P.M. Jorge, L. Lopes, J. Machado Miguens, P.J. Magalhaes Martins, A. Maio, J. Maneira, A. Morais, M. Oliveira, A. Onofre, A. Palma, J. Pina, B. Pinto, H. Santos, J.G. Saraiva, J. Silva, M. Soares, F. Veloso, H. Wolters

Republic of Belarus
Minsk AC
A. Bogouch, Y. Kulchitsky, Y.A. Kurochkin, I. Satsounkevitch, P.V. Tsiareshka

Minsk NC
V. Gilewsky, P. Kuzhir, V. Rumiantsev, P. Starovoitov, S. Yanush

Romania
Bucharest IFIN-HH
C. Alexa, E. Badescu, V. Boldea, S.I. Buda, I. Caprini, M. Caprini, C. Caramarcu, M. Ciubancan, S. Constantinescu, P. Dita, S. Dita, L. Micu, D. Pantea, G.A. Popeneciu, M. Rotaru, G. Stoicea

Politehnica Bucharest
G.L. Darlea

Timisoara WU

Russia
JINR Dubna
I.N. Aleksandrov, A. Barashkou, D.Y. Bardin, V.A. Bednyakov, I.R. Boyko, I.A. Budagov, G.A. Chelkov, A. Cheplakov, V.F. Chepurnov, M.V. Chizhov, D.V. Dedovich, M. Demichev, G.L. Glonti, M.I. Gostkin, N. Grigalashvili, Y. Gusakov, N. Huseynov, L.V. Kalinovskaya, M.Y. Kazarinov, G.D. Kekelidze, D. Kharchenko, N. Khovanskiy, E. Khramov, V. Kolesnikov, V.M. Kotov, U. Kruchonak, Z.V. Krumshteyn, V. Kukhtin, E. Ladygin, A.B. Lazarev, S. Malyukov, I.D. Manjavidze, I.A. Minashvili, M. Mineev, K. Nikolaev, A.G. Olchevski, V.D. Peshekhonov, V.M. Romanov, L. Rumyantsev, N.A. Rusakovich, R. Sadykov, A.N. Sisakyan, N.D. Topilin, V.B. Vinogradov, A. Zhemchugov

Moscow FIAN
A.V. Akimov , S.P. Baranov, I.L. Gavrilenko, A.A. Komar, R. Mashinistov, S.V. Mouraviev, P.Yu. Nechaeva, A. Shmeleva, A.A. Snesarev, V.V. Sulin, V.O. Tikhomirov

Moscow ITEP
A. Artamonov, P.A. Gorbounov, V. Khovanskiy, P.B. Shatalov, I.I. Tsukerman

Moscow MEPhI
K. Belotskiy, V.G. Bondarenko, O. Bulekov, B.A. Dolgoshein, V.A. Kantserov, S.V. Morozov, A. Romaniouk, S.Yu. Smirnov

Moscow SU
L.K. Gladilin, Y.V. Grishkevich, V.A. Kramarenko, V.I. Rud, S.Yu. Sivoklokov, L.N. Smirnova

Novosibirsk BINP
O. Beloborodova, V.B. Bobrovnikov, A. Bogdanchikov, V.A. Kazanin, G.M. Kolachev, A. Korol, V. Malyshev, A.L. Maslennikov, D.A. Maximov, I. Orlov, S.V. Peleganchuk, A.G. Schamov, K. Skovpen, A. Soukharev, A. Talyshev, Y.A. Tikhonov, A. Zaytsev

Petersburg NPI
O.L. Fedin, V. Gratchev, O.G. Grebenyuk, V.P. Maleev, S.Y. Nesterov, Y.F. Ryabov, V.A. Schegelsky, E. Sedykh, D.M. Seliverstov, Yo.K. Zalite

Protvino IHEP
V.V. Ammosov, A. Borisov, N.I. Bozhko, S.P. Denisov, R.M. Fakhrutdinov, A.B. Fenyuk, V.A. Gapienko, S.N. Golovnia, S.A. Gorokhov, V.N. Goryachev, V.N. Gushchin, A.V. Ivashin, V.V. Kabachenko, A.N. Karyukhin, A.G. Kholodenko, A.M. Kiver, S.V. Kopikov, V. Koreshev, V.A. Korotkov, A.S. Kozhin, V.V. Lapin, A.V. Larionov , M.S. Levitski, A.A. Minaenko, G.Y. Mitrofanov, A.M. Moisseev, A.G. Myagkov, V. Nikolaenko, A.V. Pleskach, V. Ryadovikov,

A.A. Solodkov, O.V. Solovyanov, E.A. Starchenko, Yu.M. Sviridov, A.P. Vorobiev, A.S. Vovenko, V.G. Zaets , A.M. Zaitsev, A.V. Zenin, O. Zenin, V.V. Zmouchko

Serbia

Belgrade IP

I. Borjanovic, J. Krstic, D.S. Popovic, D. Reljic, Dj. Sijacki, Lj. Simic, N. Vranjes, M. Vranjes Milosavljevic

Belgrade Vinca

I. Bozovic-Jelisavcic, J. Mamuzic, M. Mudrinic

Slovak Republic

Bratislava

L. Batkova, P. Federic, M. Pecsy, P. Stavina, I. Sykora, S. Tokár, T. Ženiš, B. Zilka

Kosice

J. Antos, D. Bruncko, J. Ferencei, E. Kladiva, M. Seman, P. Strizenec

Slovenia

Ljubljana

V. Cindro, I. Dolenc, A. Filipčič, A. Gorišek, B.P. Kerševan, G. Kramberger, B. Maček, I. Mandić, M. Mikuž, A. Tykhonov

South Africa

Johannesburg

Witwatersrand

K.J.C. Leney, T. Vickey

Spain

Barcelona

J. Abdallah, M. Bosman, M.P. Casado, M. Cavalli-Sforza, M.C. Conidi, B. Demirkoz, M. Dosil, X. Espinal Curull, L. Fiorini, S. Grinstein, C. Helsens, I. Korolkov, M. Martinez, E. Meoni, L.M. Mir, L. Miralles Verge, J. Nadal, C. Osuna, A. Pacheco Pages, C. Padilla Aranda, E. Perez Codina, I. Riu, V. Rossetti, E. Segura, S. Sushkov, F. Vives Vaque, M. Volpi, V. Vorwerk

Madrid UA

F. Barreiro, J. Cantero, J. Del Peso, C. Glasman, L. Labarga, T. Lagouri, L. March , E. Nebot, S. Rodier, J. Terron

Spain Granada

J.A. Aguilar-Saavedra

Valencia

G. Amorós, S. Cabrera Urbán, V. Castillo Gimenez, M.J. Costa, C. Escobar, A. Ferrer, J. Fuster, C. García, S. González de la Hoz, Y. Hernández Jiménez, E. Higón-Rodriguez, A. Irles Quiles, M. Kaci, C. Lacasta, V.R. Lacuesta, S. Marti-Garcia, M. Miñano, V.A. Mitsou, R. Moles-Valls, M. Moreno Llácer, E. Oliver Garcia, M.T. Pérez García-Estañ, E. Ros, J. Salt, C.A. Solans, U. Soldevila, J. Sánchez, E. Torró Pastor, E. Valladolid Gallego, J.A. Valls Ferrer, M. Villaplana Perez, M. Vos, A. Wildauer

Sweden

Lund

T.P.A. Åkesson, A. Alonso, J. Groth-Jensen, V. Hedberg, G. Jarlskog, B. Lundberg, E. Lytken, B. Meirose, J.U. Mjörnmark, O. Smirnova

Stockholm
B. Åsman, C. Bohm, C. Clement, D. Eriksson, K. Gellerstedt, S. Hellman, A. Hidvegi, S.O. Holmgren, M. Johansen, K.E. Johansson, K. Jon-And, J. Lesser, J. Lundberg, D.A. Milstead, T. Moa, B. Nordkvist, C.C. Ohm, A. Papadelis, M. Ramstedt, B. Sellden, S.B. Silverstein, J. Sjölin, S. Strandberg, M. Tylmad, Z. Yang

Stockholm KTH
K-J. Grahn, B. Lund-Jensen

Uppsala
C. Belanger-Champagne, R. Brenner, C.P. Buszello, T. Ekelof, M. Ellert, A. Ferrari, C.J. Hansen

Switzerland
Bern
A. Battaglia, H.P. Beck, C. Borer, A. Ereditato, T. Fonseca Martin, V. Gallo, S. Haug, S. Kabana, K. Pretzl, C. Topfel, N. Venturi, M.S. Weber

CERN
M. Aleksa, P. Amaral, F. Anghinolfi, S. Arfaoui, M.A. Baak, K. Bachas, G. Bachy, F. Baltasar Dos Santos Pedrosa, D. Banfi, M. Battistin, F. Bellina, O. Beltramello, D. Berge, F. Bertinelli, R.M. Bianchi, G. Blanchot, J.A. Bogaerts, J. Boyd, A. Braem, J. Bremer, H. Burckhart, F. Butin, S. Campana, M.D.M. Capeans Garrido, T. Carli, F. Cataneo, A. Catinaccio, A. Cattai, A. Cerri, D. Chromek-Burckhart, J. Cook, D. Côté, H.O. Danielsson, J.P. Dauvergne , M. De Oliveira Branco, A. Dell'Acqua, M. Delmastro, N. Delruelle, A. Di Girolamo, B. Di Girolamo, F. Dittus, R. Dobinson , E. Dobson, H. Drevermann, A. Dudarev, M. Dührssen , M. Dunford, F. Dydak , T. Eifert, N. Ellis, M. Elsing, C. Fabre, P. Farthouat, P. Fassnacht, I. Fedorko, J. Flammer, A. Foussat, D. Francis, S. Franz, R. Froeschl, D. Froidevaux, E. Fullana Torregrosa, C. Gabaldon, M.V. Gallas, N. Garelli, V. Garonne, J-C. Gayde, F. Gianotti, S.M. Gibson, J. Godlewski, A. Gonidec, L. Goossens, B. Gorini, P. Grafström, J. Grognuz, M. Gruwe, S. Haas, F. Hahn, S. Haider, M. Hatch, M. Hauschild, R.J. Hawkings, A.M. Henriques Correia, L. Hervas, A. Hoecker, M. Huhtinen, J. Inigo-Golfin, M.R. Jaekel, P. Jenni, O. Jonsson, C. Joram, J. Kaplon, N. Kerschen, T. Klioutchnikova, J. Knobloch, B. Koblitz, K. Köneke, T. Koffas, D. Kollar, M.J. Kotamäki, A. La Rosa, M. Lamanna, K. Lantzsch, C. Lasseur, M. Lassnig, M. Leahu, G. Lehmann Miotto, P. Lichard, L. Magnoni, A. Mapelli, L. Mapelli, J.F. Marchand, M. Marchesotti, B. Martin, J.M. Maugain, R.A. McLaren, C. Menot, A. Messina, T.C. Meyer, S. Michal, P. Miele, J. Molina-Perez, A.K. Morley, G. Mornacchi, A.M. Nairz, G. Negri, M. Nessi, B. Nicquevert, T. Niinikoski, M. Nordberg, T. Nyman, S. Palestini, Fr. Pastore, T. Pauly, R. Pengo, H. Pernegger, B.A. Petersen, J. Petersen, G. Piacquadio, O. Pirotte, K. Pommès, A. Poppleton, G. Poulard, L. Pribyl, M.J. Price, M. Raymond, C. Rembser, D. Roda Dos Santos, S. Roe, A. Salzburger, D.O. Savu, S. Schlenker, M. Schott, S. Schuh, G. Schuler, A. Sfyrla, S. Shimizu, J. Sloper, G. Spigo, R. Spiwoks, E. Stanecka, M.C. Stockton, T. Sumida, B. Szeless, K. Tackmann, G.P. Tappern, H. Ten Kate, F.J. Tique Aires Viegas, I. Torchiani, L. Tremblet, A. Tricoli, C. Tsarouchas, H. Tyrvainen, G. Unal, D. van der Ster, W. Vandelli, G. Vandoni, F. Varela Rodriguez, R. Veness, E. Vinek, R. Voss, R. Vuillermet, P.S. Wells, T. Wengler, S. Wenig, P. Werner, H.G. Wilkens, F. Winklmeier, J. Wotschack, Z. Zajacova, P.F. Zema, A. Zsenei, L. Zwalinski

Geneva
A.A. Abdelalim, G. Alexandre, M. Backes, P.J. Bell, W.H. Bell, E. Berglund, A. Blondel, F. Bucci, A. Clark, V. Dao, I. Efthymiopoulos, D. Ferrere, S. Gadomski, J.E. García Navarro, O. Gaumer, S. Gonzalez-Sevilla, M.P. Goulette, A. Hamilton, A. Leger, A. Lister, D. Macina, B. Martin dit Latour,

B. Mikulec, L. Moneta, C. Mora Herrera, M-C. Morone, S. Nektarijevic, F. Orellana, G. Pásztor , M. Pohl, A. Robichaud-Veronneau, L. Rosselet, P. Urquijo, X. Wu

Taiwan
Taipei AS
M.L. Chu, S. Hou, S.C. Lee, S.C. Lin, D. Liu, R. Mazini, Z. Meng, Z.L. Ren, D.A. Soh, P.K. Teng, J. Wang, S.M. Wang, Z. Weng, J. Zhong, Y. Zhou

Turkey
Ankara
O. Cakir, A.K. Ciftci, R. Ciftci, S. Persembe

Bogazici Istanbul
T. Akdogan, E. Arik, M. Arik, O.B. Dogan, S. Istin, V.E. Ozcan, T. Rador

Dogus
S.A. Cetin

Dumlupinar
H. Duran Yildiz

Gazi
M. Yilmaz

Gaziantep
A.J. Beddall, A. Beddall, A. Bingul, F. Diblen

Istanbul Tech U

TOBB
S. Sultansoy

Turkey Atomic EA
I. Turk Cakir

United Kingdom
Birmingham
H.S. Bansil, J. Bracinik, P.G. Bright-Thomas, D.G. Charlton, N.J. Collins, C.J. Curtis, J.D. Dowell, J. Garvey, D.R. Hadley, K. Harrison, C.M. Hawkes, S.J. Head, S.J. Hillier, J.N. Lilley, G. Mahout, T.A. Martin, T. Mclaughlan, P.R. Newman, S.W. O'Neale, J.D. Palmer, M. Slater, J.P. Thomas, P.D. Thompson, D. Typaldos, P.M. Watkins, A.T. Watson, M.F. Watson, J.A. Wilson

Cambridge
S. Ask, T. Barber, N. Barlow, J.R. Batley, F.M. Brochu, W. Buttinger, J.R. Carter, J.D. Chapman, C. Cowden, S.T. French, J.A. Frost, J.C. Hill, T.J. Khoo, C.G. Lester, V. Moeller, M.A. Parker, A.W. Phillips, D. Robinson, T. Sandoval, M. Thomson, C.P. Ward

Edinburgh
W. Bhimji, A.G. Buckley, P.J. Clark, B.J. O'Brien, B.M. Wynne

Glasgow
S.E. Allwood-Spiers, R.L. Bates, D. Britton, P. Bussey, C.M. Buttar, C. Collins-Tooth, S. D'Auria, T. Doherty, A.T. Doyle, S. Ferrag, A. Gemmell, M. Kenyon, H. McGlone, A. Moraes, V. O'Shea, C. Oropeza Barrera, A. Pickford, A. Robson, D.H. Saxon, C. Shaw, K.M. Smith, R.D. St. Denis, G. Steele, G.A. Stewart, A.S. Thompson, K. Wraight, C. Wright

Lancaster
A.E. Barton, G. Borissov, E.V. Bouhova-Thacker, T.J. Brodbeck, J.R. Catmore, S. Cheatham, A. Chilingarov, R. Davidson, L. De Mora, H. Fox, R.C.W. Henderson, G. Hughes, R.W.L. Jones, V. Kartvelishvili, R.E. Long, P.A. Love, P.N. Ratoff, T.J. Sloan, M. Smizanska, J. Walder

Liverpool
P.P. Allport, N. Austin, S. Burdin, M. D'Onofrio, P. Dervan, T. Greenshaw, C.B. Gwilliam, H.S. Hayward, M.A. Houlden, J.N. Jackson, T.J. Jones, B.T. King, M. Klein, U. Klein, T. Kluge, J. Kretzschmar, P. Laycock, S.J. Maxfield, A. Mehta, S. Migas, P.M. Prichard, G. Sellers, J.H. Vossebeld, P. Waller, C. Wiglesworth, B. Wrona

London QMUL
P. Adragna, M. Bona, A.A. Carter, L. Cerrito, E. Eisenhandler, K. Ellis, M.P.J. Landon, S.L. Lloyd, J. Morin, J.D. Morris, E. Piccaro, J. Poll, E. Rizvi, K. Stevenson, M. Teixeira Dias Castanheira, D. Traynor

London RHBNC
M.A. Alam, T. Berry, V. Boisvert, G. Boorman, N.J. Cooper-Smith, G. Cowan, C.A. Edwards, S. George, R. Gonçalo, D Hayden, G. Kilvington, A. Misiejuk, M. Rose, J.A. Strong, P. Teixeira-Dias

London UC
S. Baker, P. Bernat, S.P. Bieniek, S. Böser, J.M. Butterworth, T. Byatt, M. Campanelli, I.A. Christidi, B.D. Cooper, A.R. Davison, S. Dean, J.G. Drohan, E. Jansen, T.W. Jones, N. Konstantinidis, J. Monk, M. Nash, E. Nurse, R. Prabhu, A. Richards, J.E.M. Robinson, P. Sherwood, B. Simmons, C. Taylor, B.M. Waugh, P.A. Wijeratne

Manchester
J. Almond, G. Brown, V. Chavda, B.E. Cox, C. Da Via, I.P. Duerdoth, A. Forti, J.M. Foster, J. Howarth, R.E. Hughes-Jones, M. Ibbotson, G. Jones, J.R. Keates, M. Kelly, S.D. Kolya, J.L. Lane, F.K. Loebinger, R. Marshall, A.C. Martyniuk, M. Marx, J. Masik, P.S. Miyagawa, A. Oh, M. Owen, J.R. Pater, A.D. Pilkington, W.G. Plano, C. Schwanenberger, S.W. Snow, C.M. Tevlin, S. Watts, U.K. Yang

Oxford
A. Abdesselam, R. Apolle, A.J. Barr, P.H. Beauchemin, C.R. Boddy, N.D. Brett, J. Buchanan, R.M. Buckingham, D. Buira-Clark, P. Coe, E. Coniavitis, A.M. Cooper-Sarkar, M. Dehchar, C. Doglioni, S.M. Farrington, J. Ferrando, E.J. Gallas, L.M. Gilbert, C. Gwenlan, B.M. Hawes, A. Holmes, K. Horton, D.F. Howell, T.B. Huffman, C. Issever, M. Karagoz, R.S.B. King, G.P. Kirsch, N. Kundu, A. Larner, W. Lau, A. Lavorato, Z. Liang, S.S.A. Livermore, J. Loken , C. Mattravers, P. Mermod, R.B. Nickerson, A. Pinder, N.C. Ryder, D. Short, J.C-L. Tseng, G.H.A. Viehhauser, A.R. Weidberg, S.R. Whitehead, G. Wooden

RAL
T. Adye, J.T. Baines, B.M. Barnett, D. Botterill, S. Burke, R.W. Clifft, S.J. Dallison, A. Dewhurst, D. Emeliyanov, S.M. Fisher, B.J. Gallop, C.N.P. Gee, A.R. Gillman, D. Greenfield, S.J. Haywood, J. Kirk, N.A. McCubbin, S.J. McMahon, R.P. Middleton, W.J. Murray, P.R. Norton, P.W. Phillips, D.P.C. Sankey, W.G. Scott, J. Strube, M. Tyndel, M. Weber, F.J. Wickens, M. Wielers

Sheffield
C. Anastopoulos, C.N. Booth, P. Booth, D. Costanzo, T. Cuhadar Donszelmann, I. Dawson, R. Duxfield, M.C. Hodgkinson, P. Hodgson, P. Johansson, E.V. Korolkova, A. Mayne, J.A. Mcfayden, L. Nicolas, S. Owen, E. Paganis, M.R. Sutton, D.R. Tovey, A. Tua, D. Xu

Sussex

A. De Santo, C.J. Potter, F. Salvatore

United States of America

Albany

M.S. Alam, J. Ernst, V. Rojo

Argonne

L. Asquith, R.E. Blair, S. Chekanov, J.W. Dawson, D. Fellmann, G.F. Gieraltowski, V.J. Guarino, D. Hill, N. Hill, K. Karr, T. LeCompte, D. Malon, E.N. May, L. Nodulman, A. Paramonov, L.E. Price, J. Proudfoot, B.M. Salvachua Ferrando, J.L. Schlereth, R.W. Stanek, D.G. Underwood, P. van Gemmeren, A. Vaniachine, R. Yoshida, J. Zhang

Arizona

E. Cheu, K.A. Johns, V. Kaushik, C.L. Lampen, W. Lampl, X. Lei, P. Loch, P. Mal, F. Rühr, J.P. Rutherfoord, L. Shaver, M.A. Shupe, E.W. Varnes

Arlington UT

A. Brandt, K. De, A. Farbin, H. Kim, P. Nilsson, N. Ozturk, R. Pravahan, E. Sarkisyan-Grinbaum, M. Sosebee, B. Spurlock, A.R. Stradling, G. Usai, A. Vartapetian, A. White, J. Yu

Berkeley LBNL

J-F. Arguin, A.M. Bach, A. Barbaro Galtieri, R.M. Barnett, J. Beringer, J. Biesiada, P. Calafiura, A. Ciocio, M. Cooke, S. Dube, K. Einsweiler, R. Ely, A. Gaponenko, M. Garcia-Sciveres, M. Gilchriese, C. Haber, B. Heinemann, I. Hinchliffe, S.-C. Hsu, M. Hurwitz, J. Joseph, A. Korn, W. Lavrijsen, C. Leggett, P. Loscutoff, J. Lys, R.J. Madaras, D.R. Quarrie, C. Ruwiedel, M.I. Scherzer, M. Shapiro, J. Siegrist, L.A. Skinnari, G. Stavropoulos, M. Tatarkhanov, L. Tompkins, S. Vahsen, D. Varouchas, J. Virzi, W-M. Yao, Y. Yao, S. Zenz

Boston

S.P. Ahlen, K.M. Black, J.M. Butler, R.D. Harrington, E. Hazen, M. Lewandowska, J. Love, A. Marin, N.R. Nation, C. Posch, J.T. Shank, S.P. Whitaker, Z. Yan, S. Youssef

Brandeis

S. Aefsky, C. Amelung, J.R. Bensinger, C. Blocker, L.E. Kirsch, D. Pomeroy, N. Skvorodnev, H. Wellenstein

Brookhaven BNL

D.L. Adams, K. Assamagan, M.D. Baker, M. Begel, H. Chen, V. Chernyatin, P.E. De Castro Faria Salgado, M. Ernst, T. Gadfort, B. Gibbard, H.A. Gordon, R. Hackenburg, A. Klimentov, F. Lanni, D. Lissauer, D. Lynn, H. Ma, T. Maeno, S. Majewski, P. Nevski, K. Nikolopoulos, D. Oliveira Damazio, F. Paige, S. Panitkin, M.-A. Pleier, A. Poblaguev, V. Polychronakos, S. Protopopescu, C. Rahm, S. Rajagopalan, G. Redlinger, S. Snyder, J. Sondericker, P. Steinberg, I. Stumer, H. Takai, F. Tarrade, A. Undrus, T. Wenaus, S. White, S. Ye, D. Yu

Chicago

K.J. Anderson, A. Boveia, E. Brubaker, F. Canelli, G. Choudalakis, T. Costin, E.J. Feng, M. Fiascaris, R.W. Gardner, A. Gupta, I. Jen-La Plante, A. Kapliy, C. Melachrinos, F.S. Merritt, P.U.E. Onyisi, M.J. Oreglia, J.E. Pilcher, M.J. Shochet, J.M. Tuggle

Columbia

T. Andeen, A. Angerami, G. Brooijmans, K. Copic, J. Dodd, N. Grau, H.M. Gray, J. Guo, E.W. Hughes, M. Leltchouk, D. Lopez Mateos, Z. Marshall, J.A. Parsons, A. Penson, K. Perez, V. Perez Reale, F. Spanò, P.M. Tuts, D. Urbaniec, E. Williams, W. Willis, E. Wulf, L. Živković

Dallas SMU

R.K. Daya, K. Dindar Yagci, A. Firan, D. Goldin, H.K. Hadavand, J. Hoffman, Y. Ilchenko, R. Ishmukhametov, D. Joffe, S. Kama, A. Kasmi, R. Kehoe, Z. Liang, L. Lu, P. Renkel, R.R. Rios, R. Stroynowski, J. Ye, P. Zarzhitsky

Dallas UT
M. Ahsan, E. Galyaev, J.M. Izen, X. Lou, K. Reeves

Duke
A.T.H. Arce, D.P. Benjamin, A. Bocci, W.L. Ebenstein, A.J. Fowler, B.R. Ko, S.H. Oh, C. Wang, J. Yamaoka

Fresno
H.S. Bawa, Y.S. Gao, A.J. Lowe

Hampton
T.N. Addy, A. Harvey, K.W. McFarlane, T. Shin, V.I. Vassilakopoulos

Harvard
J. Barreiro Guimarães da Costa, A. Belloni, G.W. Brandenburg, M. Franklin, P. Hurst, J. Huth, L. Jeanty, M. Kagan, V. Martinez Outschoorn, C. Mills, S. Moed, M. Morii, S. Prasad, B.C. Smith, G. Zevi della Porta

Indiana
S. Brunet, P. Cwetanski, H. Evans, P. Gagnon, V. Jain, F. Luehring, C.P. Marino, H. Ogren, J. Penwell, D. Price, D.R. Rust, D. Whittington, Y. Yang, D. Zieminska

Iowa
P.K. Behera, M. Limper, U. Mallik, R. Zaidan

Iowa State
J. Cochran, F. Dudziak, A. Lebedev, A.S. Mete, W.T. Meyer, A. Nelson, S. Prell, E.I. Rosenberg, A. Ruiz-Martinez, N. Triplett, K. Yamamoto

Louisiana Tech
C. Bernius, R. Dhullipudi, Z.D. Greenwood, L. Sawyer, M.C. Tamsett

Louisville

Massachusetts
B. Brau, G. Colon, C. Dallapiccola, A. Meade, E.J.W. Moyse, E.N. Thompson, N. van Eldik, S. Willocq, M.J. Woudstra

Michigan
A.J. Armbruster, J.W. Chapman, M. Cirilli, T. Dai, E.B. Diehl, A. Eppig, C. Ferretti, S. Goldfarb, D. Harper, D. Levin, X. Li, H. Liu, J.B. Liu, S.P. Mc Kee, H.A. Neal, N. Panikashvili, J. Purdham, J. Qian, D. Scheirich, J. Strandberg, R.P. Thun, S. Walch, A. Wilson, H. Yang, B. Zhou

Michigan SU
M. Abolins, G. Arabidze, R. Brock, C. Bromberg, S. Caughron, G. Comune, A. Di Mattia, W. Fedorko, R. Hauser, S. Heim, J.L. Holzbauer, J. Huston, J. Koll, J. Kraus, J.T. Linnemann, P.S. Mangeard, B. Martin, R.J. Miller, B.G. Pope, P. Ryan, R. Schwienhorst, K. Tollefson, H. Zhang

MIT
F.E. Taylor

New Mexico
I. Gorelov, M.R. Hoeferkamp, J. Metcalfe, S.C. Seidel, K. Toms, R. Wang

Northern Illinois
R. Calkins, D. Chakraborty, J.G. Rocha de Lima, C. Suhr, V. Zutshi

NYU New York
B. Budick, D. Casadei, K. Cranmer, R. Djilkibaev, L. Hooft van Huysduynen, R. Konoplich, A. Krasznahorkay, G.H. Lewis, A.I. Mincer, P. Nemethy, R.M. Neves, K. Prokofiev, A. Shibata, L. Zhao

Ohio SU
W. Fernando, M.J. Fisher, K.K. Gan, H. Kagan, R.D. Kass, J. Moss, A.M. Rahimi, M. Strang

Oklahoma
B. Abbott, P. Gutierrez, G.S. Huang, D.K. Jana, A. Marzin, R. Meera-Lebbai, M. Saleem, H. Severini, P. Skubic, J. Snow, M. Strauss

Oklahoma SU
B. Abi, A. Khanov, F. Rizatdinova

Oregon
J.E. Brau, E. Ptacek, A. Reinsch, M. Robinson, J. Searcy, M. Shamim, N.B. Sinev, D.M. Strom, E. Torrence

Pennsylvania
J. Alison, J. Degenhardt, M. Donega, N. Dressnandt, S. Fratina, M. Hance, E. Hines, B. Jackson, J. Kroll, J. Kunkle, B.C. LeGeyt, E. Lipeles, F.F. Martin, D. Olivito, R. Ospanov, R. Reece, J. Stahlman, E. Thomson, P. Wagner, H.H. Williams

Pittsburgh
J. Boudreau, C. Boulahouache, W. Cleland, T. Kittelmann, J. Mueller, V. Paolone, D. Prieur, V. Savinov, V. Tsulaia, S. Wendler, R. Yoosoofmiya

Santa Cruz UC
A. Bangert, S. Chouridou, D.S. Damiani, T. Dubbs, K. Fowler, A.A. Grillo, G.A. Hare, A.M. Litke, W.S. Lockman, P.M. Manning, J. Mitrevski, J. Nielsen, H.F-W. Sadrozinski, B.A. Schumm, A. Seiden

Seattle Washington
D.A. Forbush, A.G. Goussiou, J. Griffiths, O.M. Harris, W. Kuykendall, H.J. Lubatti, P. Mockett, A. Policicchio, S. Rosati, J. Rothberg, D. Ventura, M. Verducci, J.C. Wang, G. Watts, T. Zhao

SLAC
I. Aracena, T. Barklow, R. Bartoldus, B. Butler, J.G. Cogan, P. Grenier, A. Haas, P. Hansson, C. Horn, P. Jackson, P.C. Kim, M. Kocian, T. Koi, D.W. Miller, R. Mount, S. Nelson, T.K. Nelson, A. Salnikov, A. Schwartzman, D. Silverstein, D. Smith, E. Strauss, D. Su, M.G. Wilson, M. Wittgen, C. Young

South Carolina
W. Park, M. Purohit, A. Trivedi

Stony Brook
A. Ahmad, R. Caputo, C. Deluca, E. Devetak, B. DeWilde, R. Engelmann, J. Farley, J.J. Goodson, V. Grassi, J.A. Gray, J. Hobbs, J. Jia, A. Khodinov, R.L. McCarthy, S. Mohapatra, M. Rijssenbeek, R.D. Schamberger, J. Stupak, D. Tsybychev, A. Yurkewicz

Tufts
S. Hamilton, A. Napier, S. Rolli, K. Sliwa, S. Todorova-Nova

UC Irvine

B.H. Benedict, T. Bold, M.D. Ciobotaru, J. Deng, M. Dobson, I. Gough Eschrich, I. Grabowska-Bold, D. Hawkins, A.J. Lankford, H. Okawa, R. Porter, D.A. Scannicchio, A. Taffard, B. Toggerson, G. Unel, M. Werth, S.J. Wheeler-Ellis, D. Whiteson, N. Zhou

UI Urbana
N. Benekos, J. Coggeshall, A. Cortes-Gonzalez, D. Errede, S. Errede, H. Khandanyan, K. Lie, T.M. Liss, A. McCarn, M.S. Neubauer, I. Vichou

Wisconsin
R. Asfandiyarov, G.D. Carrillo Montoya, A.M. Castaneda Hernandez, E. Castaneda-Miranda, X. Chen, A. Dos Anjos, Y. Fang, D. Fasching, L.R. Flores Castillo, S. Gonzalez, O. Gutzwiller, H. Ji, L. Kashif, A. Leung Fook Cheong, H. Li, L.L. Ma, B.R. Mellado Garcia, Y.B. Pan, S. Pataraia, M.I. Pedraza Morales, H. Peng, J. Poveda, W.B. Quayle, T. Sarangi, H. Wang, W. Wiedenmann, S.L. Wu, Y. Zhu, G. Zobernig

Yale
J. Adelman, G. Atoian, B. Auerbach, O.K. Baker, C. Cuenca Almenar, S. Demers, F. Garberson, T. Golling, D. Guest, P.J. Hsu, B. Kaplan, L. Lee, S. Lockwitz, A. Loginov, A.J. Martin, M.P. Schmidt, D. Sherman, M. Thioye, P. Tipton, R. Wall, M. Zeller